

# We are IntechOpen, the world's leading publisher of Open Access books Built by scientists, for scientists

6,900

Open access books available

186,000

International authors and editors

200M

Downloads

Our authors are among the

154

Countries delivered to

TOP 1%

most cited scientists

12.2%

Contributors from top 500 universities



WEB OF SCIENCE™

Selection of our books indexed in the Book Citation Index  
in Web of Science™ Core Collection (BKCI)

Interested in publishing with us?  
Contact [book.department@intechopen.com](mailto:book.department@intechopen.com)

Numbers displayed above are based on latest data collected.  
For more information visit [www.intechopen.com](http://www.intechopen.com)



## Evolution of Phases in a Recycled Al-Si Cast Alloy During Solution Treatment

Eva Tillová, Mária Chalupová and Lenka Hurtalová  
*University of Žilina,  
 Slovak Republic*

### 1. Introduction

Aluminium has been acquiring increasing significance for the past few decades due to its excellent properties and diversified range of applications. Aluminium has been recognized as one of the best candidate materials for various applications by different sectors such as automotive, construction, aerospace, etc. The increasing demand for aluminium-based products and further globalization of the aluminium industry have contributed significantly to the higher consumption of aluminium scrap for re-production of aluminium alloys (Mahfoud et al., 2010).

Secondary aluminium alloys are made out of aluminium scrap and workable aluminium garbage by recycling. Production of aluminium alloys belong to heavy source fouling of life environs. Care of environment in industry of aluminium connects with the decreasing consumptions resource as energy, materials, waters and soil, with increase recycling and extension life of products. More than half aluminium on the present produce in European Union comes from recycled raw material. By primary aluminium production we need a lot of energy and constraints decision mining of bauxite so European Union has big interest of share recycling aluminium, and therefore increase interest about secondary aluminium alloys and cast stock from them (Sencakova & Vircikova, 2007).

The increase in recycled metal becoming available is a positive trend, as secondary aluminium produced from recycled metal requires only about 2.8 kWh/kg of metal produced while primary aluminium production requires about 45 kWh/kg produced. It is to the aluminium industry's advantage to maximize the amount of recycled metal, for both the energy-savings and the reduction of dependence upon overseas sources. The remelting of recycled metal saves almost 95 % of the energy needed to produce prime aluminium from ore, and, thus, triggers associated reductions in pollution and greenhouse emissions from mining, ore refining, and melting. Increasing the use of recycled metal is also quite important from an ecological standpoint, since producing aluminium by recycling creates only about 5 % as much CO<sub>2</sub> as by primary production (Das, 2006; Das & Gren, 2010).

Today, a large amount of new aluminium products are made by recycled (secondary) alloys. This represents a growing "energy bank" of aluminium available for recycling at the end of components' lives, and thus recycling has become a major issue. The future growth offers an

opportunity for new recycling technologies and practices to maximize scrap quality; improve efficiency and reduce cost.

Aluminium-silicon (Al-Si) cast alloys are fast becoming the most universal and popular commercial materials, comprising 85 % to 90 % of the aluminium cast parts produced for the automotive industry, due to their high strength-to-weight ratio, excellent castability, high corrosion resistant and chemical stability, good mechanical properties, machinability and wear resistance. Mg or Cu addition makes Al-Si alloy heat treatable.

The alloys of the Al-Si-Cu system have become increasingly important in recent years, mainly in the automotive industry that uses recycled (secondary) aluminium in the form of various motor mounts, pistons, cylinder heads, heat exchangers, air conditioners, transmissions housings, wheels, fenders and so on due to their high strength at room and high temperature (Rios & Caram, 2003; Li et al., 2004; Michna et al., 2007). The increased use of these recycled alloys demands a better understanding of its response to mechanical properties.

The quality of recycled Al-Si casting alloys is considered to be a key factor in selecting an alloy casting for a particular engineering application. Based on the Al-Si system, the main alloying elements are copper (Cu) or magnesium (Mg) and certain amount of iron (Fe), manganese (Mn) and more, that are present either accidentally, or they are added deliberately to provide special material properties. These elements partly go into solid solution in the matrix and partly form intermetallic particles during solidification. The size, volume and morphology of intermetallic phases are functions of chemistry, solidification conditions and heat treatment (Li, 1996; Paray & Gruzleski, 1994; Tillova & Panuskova, 2007, 2008).

Copper substantially improves strength and hardness in the as-cast and heat-treated conditions. Alloys containing 4 % to 6 % Cu respond most strongly to thermal treatment. Copper generally reduces resistance to general corrosion and, in specific compositions and material conditions, stress corrosion susceptibility. Additions of copper also reduce hot tear resistance and decrease castability. Magnesium is the basis for strength and hardness development in heat-treated Al-Si alloys too and is commonly used in more complex Al-Si alloys containing copper, nickel, and other elements for the same purpose.

Iron considers the principal impurity and detrimental alloying element for Al-Si-Cu alloys. Iron improves hot tear resistance and decreases the tendency for die sticking or soldering in die casting. Increases in iron content are, however, accompanied by substantially decreased ductility. Iron reacts to form a myriad of insoluble phases in aluminium alloy melts, the most common of which are  $\text{Al}_3\text{Fe}$ ,  $\text{Al}_6\text{FeMn}$ , and  $\alpha\text{-Al}_5\text{FeSi}$ . These essentially insoluble phases are responsible for improvements in strength, especially at elevated temperature. As the fraction of insoluble phase increases with increased iron content, casting considerations such as flowability and feeding characteristics are adversely affected. Iron also lead to the formation of excessive shrinkage porosity defects in castings (Warmuzek, 2004a; Taylor, 2004; Shabestari, 2004; Caceres et al., 2003; Wang et al. 2001; Tillova & Chalupova, 2010).

It is clear that the morphology of Fe-rich intermetallic phases influences harmfully also fatigue properties (Taylor, 2004; Tillova & Chalupova, 2010). It is recognized that recycled Al-Si-Cu alloys are not likely to be suitable for fracture-critical components, where higher levels of Fe and Si have been shown to degrade fracture resistance. However the likelihood

exists that they may perform quite satisfactorily in applications such as those listed where service life is determined by other factors (Taylor, 2004).

2. Experimental material and methodology

As an experimental material recycled (secondary) hypoeutectic AlSi9Cu3 alloy, in the form of 12.5 kg ingots, was used. The alloy was molten into the sand form (sand casting). The melting temperature was maintained at 760 °C ± 5 °C. Molten metal was before casting purified with salt AlCu4B6. The melt was not modified or grain refined. The chemical analysis of AlSi9Cu3 cast alloy was carried out using arc spark spectroscopy. The chemical composition is given in the table 1.

Si	Cu	Mn	Fe	Mg	Ni	Pb	Zn	Ti	Al
10.7	2.4	0.22	< 0.8	0.47	0.08	0.11	1.1	0.03	rest

Table 1. Chemical composition of the alloy (wt. %)

AlSi9Cu3 cast alloy has lower corrosion resistance and is suitable for high temperature applications (dynamic exposed casts, where are not so big requirements on mechanical properties) - it means to max. 250 °C. Experimental samples (standard tensile test specimens) were given a T4 heat treatment - solution treatment for 2, 4, 8, 16 or 32 hours at three temperatures (505 °C, 515 °C and 525 °C); water quenching at 40 °C and natural aging for 24 hours at room temperature. After heat treatment samples were subjected to mechanical test. For as cast state, each solution temperature and each aging time, a minimum of five specimens were tested.

Metallographic samples were prepared from selected tensile specimens (after testing) and the microstructures were examined by optical (Neophot 32) and scanning electron microscopy. Samples were prepared by standards metallographic procedures (mounting in bakelite, wet ground, DP polished with 3 µm diamond pastes, finally polished with commercial fine silica slurry (STRUERS OP-U) and etched by Dix-Keller. For setting of Fe-rich intermetallic phases was used etching by H2SO4. For setting of Cu-rich intermetallic phases was used etching by HNO3.

Some samples were also deep-etched for 30 s in HCl solution in order to reveal the three-dimensional morphology of the eutectic silicon and intermetallic phases (Tillova & Chalupova, 2001, 2009). The specimen preparation procedure for deep-etching consists of dissolving the aluminium matrix in a reagent that will not attack the eutectic components or intermetallic phases. The residuals of the etching products should be removed by intensive rinsing in alcohol. The preliminary preparation of the specimen is not necessary, but removing the superficial deformed or contaminated layer can shorten the process. To determine the chemical composition of the intermetallic phases was employed scanning electron microscopy (SEM) TESCAN VEGA LMU with EDX analyser BRUKER QUANTAX.

Quantitative metallography (Skocovsky & Vasko, 2007; Vasko & Belan, 2007; Belan, 2008; Vasko, 2008; Martinkovic, 2010) was carried out on an Image Analyzer NIS - Elements 3.0 to quantify phase’s changes during heat treatment. A minimum of 20 pictures at 500 x magnification of the polish per specimen were taken.

Hardness measurement was preformed by a Brinell hardness tester with a load of 62.5 kp, 2.5 mm diameter ball and a dwell time of 15 s. The Brinell hardness value at each state was obtained by an average of at least six measurements. The phases Vickers microhardness was measured using a MHT-1 microhardness tester under a 1g load for 10 s (HV 0.01). Twenty measurements were taken per sample and the median microhardness was determined.

3. Results and discussion

3.1 Microstructure of recycled AlSi9Cu3 cast alloy

Controlling the microstructure during solidification is, therefore, very important. The Al-Si eutectic and intermetallic phases form during the final stage of the solidification. How the eutectic nucleates and grows have been shown to have an effect on the formation of defects such as porosity and microporosity too. The defects, the morphology of eutectic and the morphology of intermetallic phases have an important effect on the ultimate mechanical properties of the casting.

As recycling of aluminium alloys becomes more common, sludge will be a problem of increasing importance due to the concentration of Fe, Mn, Cr and Si in the scrap cycle. During the industrial processing of the Al-Si alloys, these elements go into solid solution but they also form different intermetallic phases. The formation of these phases should correspond to successive reaction during solidification - table 2 (Krupiński et al., 2011; Maniara et al., 2007; Mrówka-Nowotnik & Sieniawski, 2011; Dobrzański et al., 2007, Tillova & Chalupova, 2009). Thus, control of these phases e. g. quantitative analysis (Vasko & Belan, 2007; Martinkovic, 2010) is of considerable technological importance. Typical structures of the recycled as-cast AlSi9Cu3 alloys are shown in Fig. 1. The microstructure consists of dendrites  $\alpha$ -phase (1), eutectic (mixture of  $\alpha$ -matrix and spherical Si-phases - 2) and variously type's intermetallic Fe- and Cu-rich phases (3 and 4).

Reactions	Temperature, °C
$\alpha$ - dendritic network	609
$Liq. \rightarrow \alpha - phase + Al_{15}Mn_3Si_2 + Al_5FeSi$	590
$Liq. \rightarrow \alpha - phase + Si + Al_5FeSi$	575
$Liq. \rightarrow \alpha - phase + Al_2Cu + Al_5FeSi + Si$	525
$Liq. \rightarrow \alpha - phase + Al_2Cu + Si + Al_5Mg_8Si_6Cu_2$	507

Table 2. Reactions occurring during the solidification of AlSi9Cu3 alloys

The  $\alpha$ -matrix precipitates from the liquid as the primary phase in the form of dendrites and is nominally comprised of Al and Si. Experimental material was not modified and so eutectic Si particles are in a form of platelets (Fig. 2a), which on scratch pattern are in a form of needles – Fig. 2b (Skocovsky et al., 2009; Tillova & Chalupova, 2001; 2009).

Iron is one of the most critical alloying elements, because Fe is the most common and usually detrimental impurity in cast Al-Si alloys. Iron impurities can either come from the use of steel tools or scrap materials or be acquired during subsequent melting, remelting and casting, e.g. by contamination from the melting pot etc.



A number of Fe-rich intermetallic phases, including  $\alpha$  ( $\text{Al}_8\text{Fe}_2\text{Si}$  or  $\text{Al}_{15}(\text{FeMn})_3\text{Si}_2$ ),  $\beta$  ( $\text{Al}_5\text{FeSi}$ ),  $\pi$  ( $\text{Al}_8\text{Mg}_3\text{FeSi}_6$ ), and  $\delta$  ( $\text{Al}_4\text{FeSi}_2$ ), have been identified in Al-Si cast alloys (Samuel et al., 1996; Taylor, 2004; Seifeddine, 2007; Seifeddine et al. 2008; Moustafa, 2009; Fang et al., 2007; Lu & Dahle, 2005).

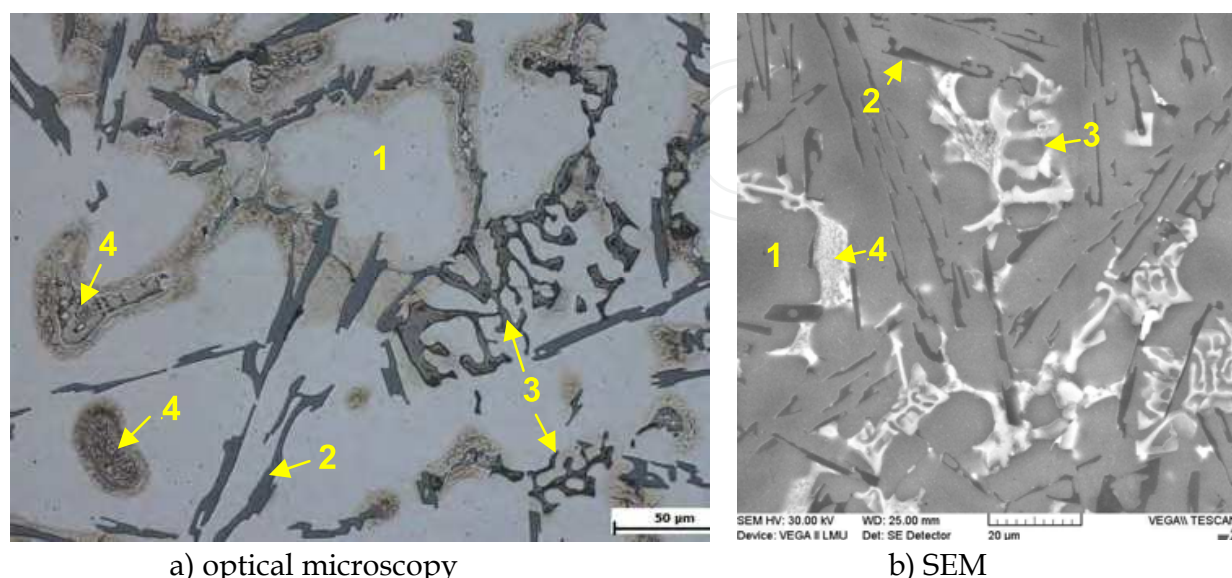


Fig. 1. Microstructure of recycled AlSi9Cu3 cast alloy (1 –  $\alpha$ -phase, 2 – eutectic silicon, 3 – Fe-rich phases, 4 – Cu-rich phases), etch. Dix-Keller

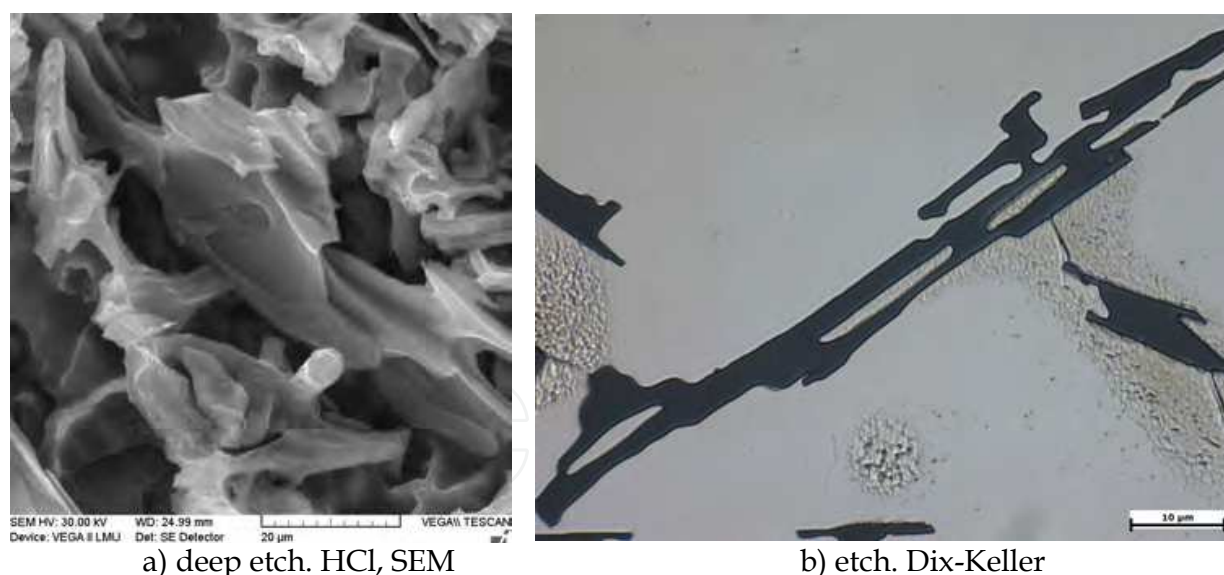


Fig. 2. Morphology of eutectic silicon

In experimental AlSi9Cu3 alloy was observed the two main types of Fe-rich intermetallic phases,  $\text{Al}_5\text{FeSi}$  with monoclinic crystal structure (know as beta- or  $\beta$ -phase) and  $\text{Al}_{15}(\text{FeMn})_3\text{Si}_2$  (know as alpha- or  $\alpha$ -phase) with cubic crystal structure. The first phase ( $\text{Al}_5\text{FeSi}$ ) precipitates in the interdendritic and intergranular regions as platelets (appearing as needles in the metallographic microscope - Fig. 3). Long and brittle  $\text{Al}_5\text{FeSi}$  platelets (more than 500  $\mu\text{m}$ ) can adversely affect mechanical properties, especially ductility, and also

lead to the formation of excessive shrinkage porosity defects in castings (Caceres et al., 2003). Platelets are effective pore nucleation sites. It was also shown that the  $\text{Al}_5\text{FeSi}$  needles can act as nucleation sites for Cu-rich  $\text{Al}_2\text{Cu}$  phases (Tillova et al., 2010).

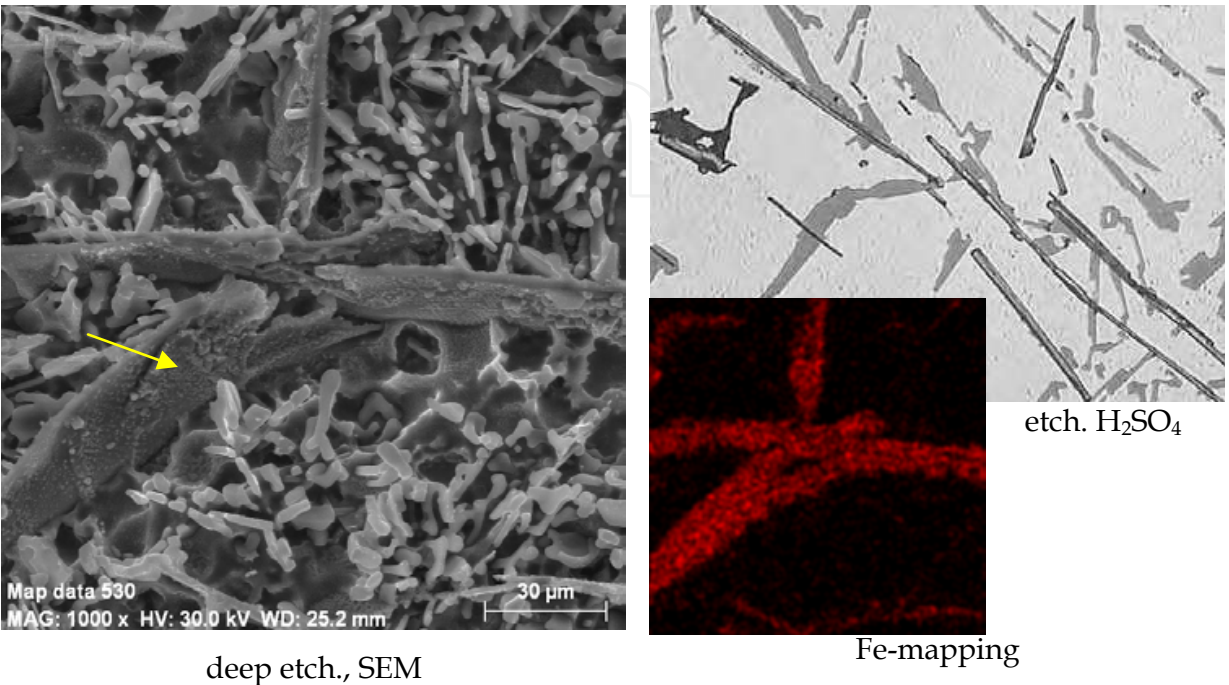


Fig. 3. Morphology of Fe-phase  $\text{Al}_5\text{FeSi}$

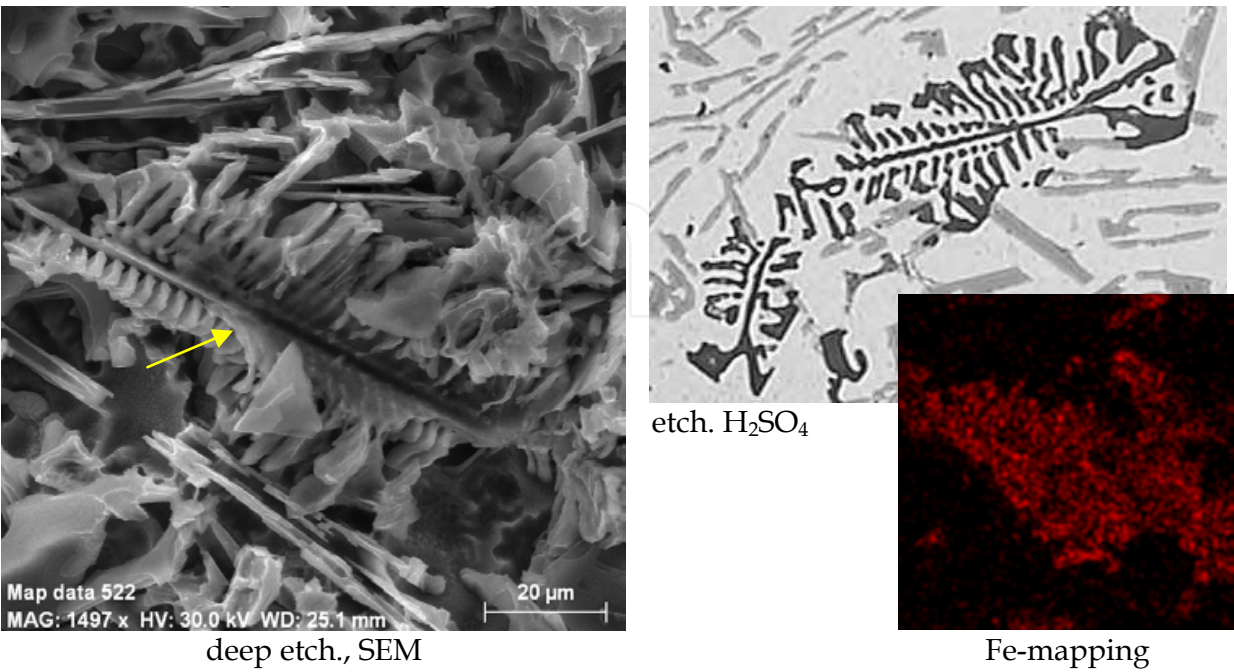


Fig. 4. Morphology of Fe-phase  $\text{Al}_{15}(\text{FeMn})_3\text{Si}_2$

The deleterious effect of  $\text{Al}_5\text{FeSi}$  can be reduced by increasing the cooling rate, superheating the molten metal, or by the addition of a suitable “neutralizer” like Mn, Co, Cr, Ni, V, Mo and Be. The most common addition has been manganese. Excess Mn may reduce  $\text{Al}_5\text{FeSi}$  phase and promote formation Fe-rich phases  $\text{Al}_{15}(\text{FeMn})_3\text{Si}_2$  in form „skeleton like“ or in form „Chinese script“ (Seifeddine et al., 2008; Taylor, 2004) (Fig. 4). This compact morphology “Chinese script” (or skeleton - like) does not initiate cracks in the cast material to the same extent as  $\text{Al}_5\text{FeSi}$  does and phase  $\text{Al}_{15}(\text{FeMn})_3\text{Si}_2$  is considered less harmful to the mechanical properties than  $\beta$  phase (Ma et al., 2008; Kim et al., 2006). The amount of manganese needed to neutralize iron is not well established. A common “rule of thumb” appears to be ratio between iron and manganese concentration of 2:1.

Alloying with Mn and Cr, caution has to be taken in order to avoid the formation of hard complex intermetallic multi-component sludge,  $\text{Al}_{15}(\text{FeMnCr})_3\text{Si}_2$  - phase (Fig. 5). These intermetallic compounds are hard and can adversely affect the overall properties of the casting. The formation of sludge phases is a temperature dependent process in a combination with the concentrations of iron, manganese and chromium independent of the silicon content. If Mg is also present with Si, an alternative called pi-or  $\pi$ -phase can form,  $\text{Al}_5\text{Si}_6\text{Mg}_8\text{Fe}_2$ .  $\text{Al}_5\text{Si}_6\text{Mg}_8\text{Fe}_2$  has a script-like morphology. The Fe-rich particles can be twice as large as the Si particles, and the cooling rate has a direct impact on the kinetics, quantities and size of Fe-rich intermetallic present in the microstructure.

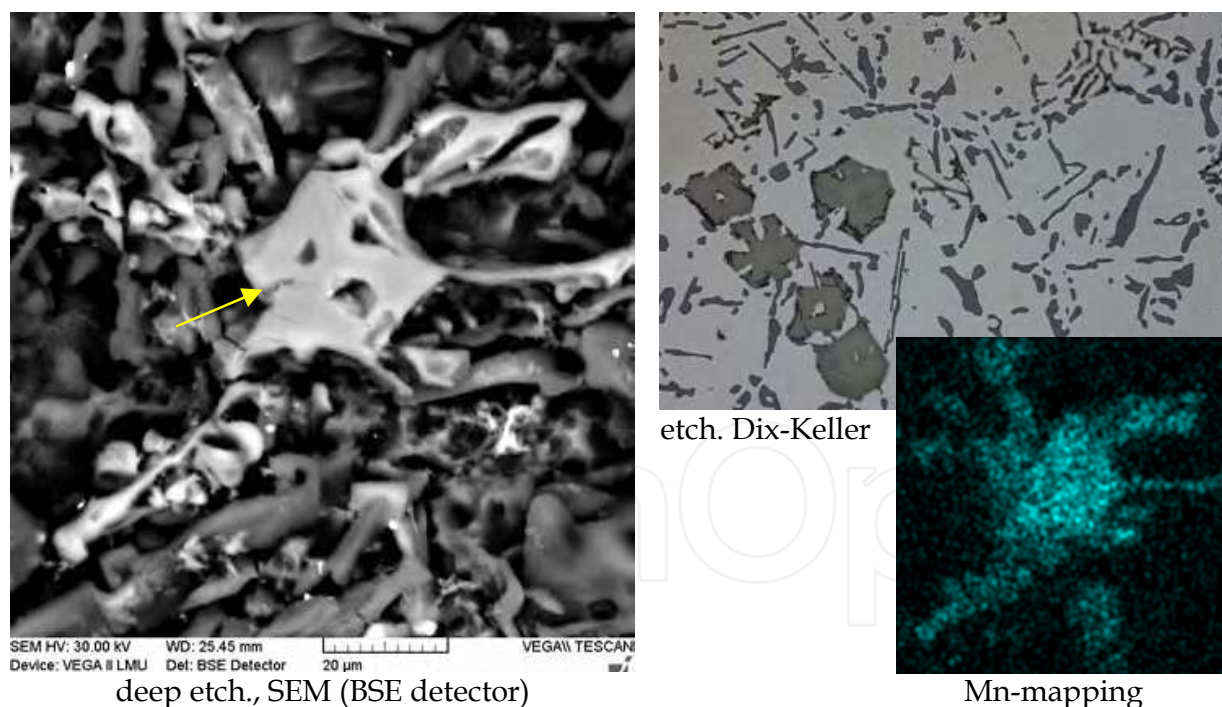


Fig. 5. Morphology of sludge phase  $\text{Al}_{15}(\text{FeMnCr})_3\text{Si}_2$

Cu is in Al-Si-Cu cast alloys present primarily as phases:  $\text{Al}_2\text{Cu}$ , Al- $\text{Al}_2\text{Cu}$ -Si or  $\text{Al}_5\text{Mg}_8\text{Cu}_2\text{Si}_6$  (Rios et al., 2003; Tillova & Chalupova, 2009; Tillova et al.; 2010). The average size of the Cu-phase decreases upon Sr modification. The  $\text{Al}_2\text{Cu}$  phase is often observed to precipitate both in a small blocky shape with microhardness 185 HV 0.01. Al- $\text{Al}_2\text{Cu}$ -Si phase is observed in very fine multi-phase eutectic-like deposits with microhardness 280 HV 0.01



(Tillova & Chalupova, 2009). In recycled AlSi9Cu3 alloy was analysed two Cu-phases: Al<sub>2</sub>Cu and Al-Al<sub>2</sub>Cu-Si (Fig. 6).

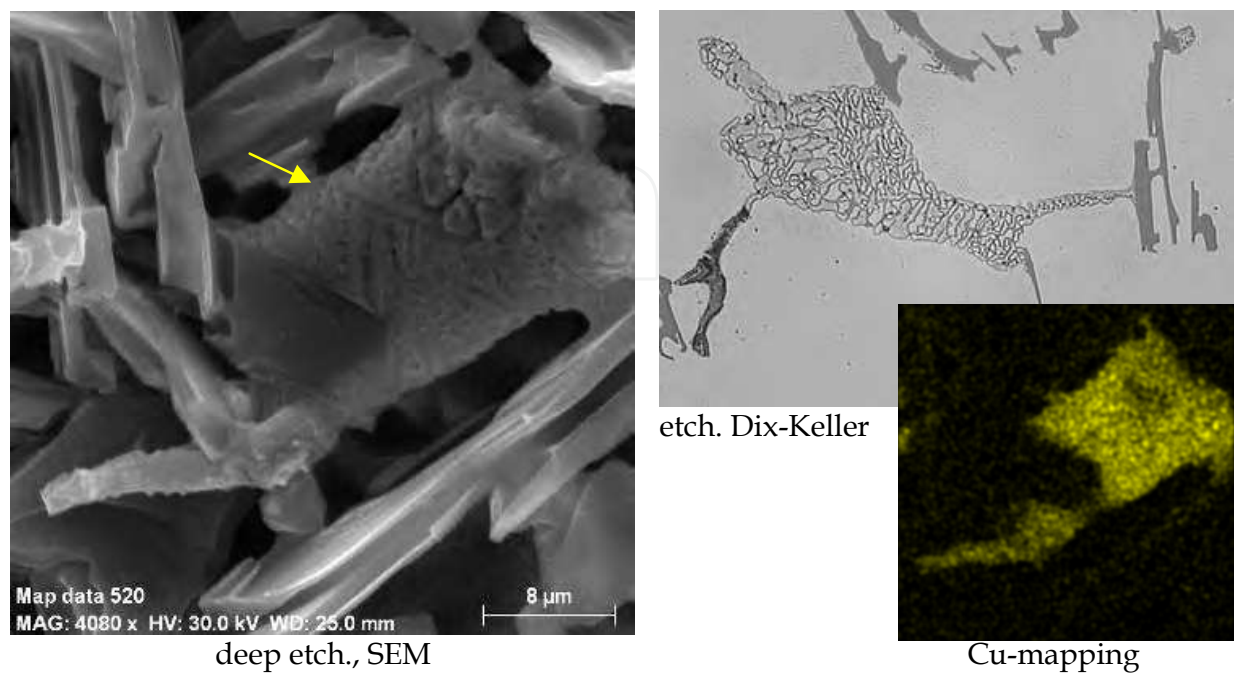


Fig. 6. Morphology of Cu-phase - Al-Al<sub>2</sub>Cu-Si

The microhardness of all observed intermetallic phases was measured in HtW Dresden and the microhardness values are indicated in table 3. It is evident that the eutectic silicon, the Fe-rich phase Al<sub>5</sub>FeSi and the multicomponent intermetallic Al<sub>15</sub>(FeMn)<sub>3</sub>Si<sub>2</sub> are the hardest.

Intermetallic phases	HV 0.01	Chemical composition, wt. %					
		Al	Mg	Si	Fe	Cu	Mn
Al <sub>15</sub> (MnFe) <sub>3</sub> Si <sub>2</sub>	483	61	-	10.3	13.4	2.6	13.6
Al <sub>5</sub> FeSi	1 475	67.7	-	16.5	15.8	-	-
Al <sub>2</sub> Cu	185	53.5	-	-	-	42.2	-
Al-Al <sub>2</sub> Cu-Si	280	53	4.5	14.8	-	18.5	-
Si	1084	-	-	99.5	-	-	-

Table 3. Microhardness and chemical composition of intermetallic phases

Influence of intermetallic phases to mechanical and fatigue properties of recycled Al-Si cast alloys depends on size, volume and morphology this Fe- and Cu-rich phases.

3.2 Effect of solution treatment on the mechanical properties

Al-Si-Cu cast alloys are usually heat-treated in order to obtain an optimum combination of strength and ductility. Important attribute of a precipitation hardening alloy system is a temperature and time dependent equilibrium solid-solubility characterized by decreasing solubility with decreasing temperature and then followed by solid-state precipitation of

second phase atoms on cooling in the solidus region (Abdulwahab, 2008; Michna et al., 2007; ASM Handbook, 1991). Hardening heat treatment involves (Fig. 7):

- Solution heat - treatment - it is necessary to produce a solid solution. Production of a solid solution consists of soaking the aluminium alloy at a temperature sufficiently high and for such a time so as to attain an almost homogeneous solid solution;
- Rapid quenching to retain the maximum concentration of hardening constituent ( $\text{Al}_2\text{Cu}$ ) in solid solution. By quenching it is necessary to avoid slow cooling. Slow cooling can may the precipitation of phases that may be detrimental to the mechanical properties. For these reasons solid solutions formed during solution heat-treatment are quenched rapidly without interruption to produce a supersaturated solution at room temperature;
- Combination of artificial and over-ageing to obtain the desired mechanical properties in the casting. Generally artificial aging imparts higher strength and hardness values to aluminium alloys without sacrificing other mechanical properties.

The precipitation sequence for Al-Si-Cu alloy is based upon the formation of  $\text{Al}_2\text{Cu}$  based precipitates. The sequence is described as:  $\alpha_{ss} \rightarrow \text{GP zones} \rightarrow \theta' \rightarrow \theta (\text{Al}_2\text{Cu})$ . The sequence begins upon aging when the supersaturated solid solution ( $\alpha_{ss}$ ) gives way first to small coherent precipitates called GP zones. These particles are invisible in the optical microscope but macroscopically, this change is observed as an increase in the hardness and tensile strength of the alloy. As the process proceeds, the GP zones start to dissolve, and  $\theta'$  begins to form, which results in a further increase in the hardness and tensile strength in the alloy. Continued aging causes the  $\theta'$  phase to coarsen and the  $\theta (\text{Al}_2\text{Cu})$  precipitate to appear. The  $\theta$  phase is completely incoherent with the matrix, has a relatively large size, and has a coarse distribution within the aluminium matrix. Macroscopically, this change is observed as an increase in the ductility and a decrease in the hardness and tensile strength of the alloy (Abdulwahab, 2008; Michna et al., 2007; Panuskova et al., 2008).

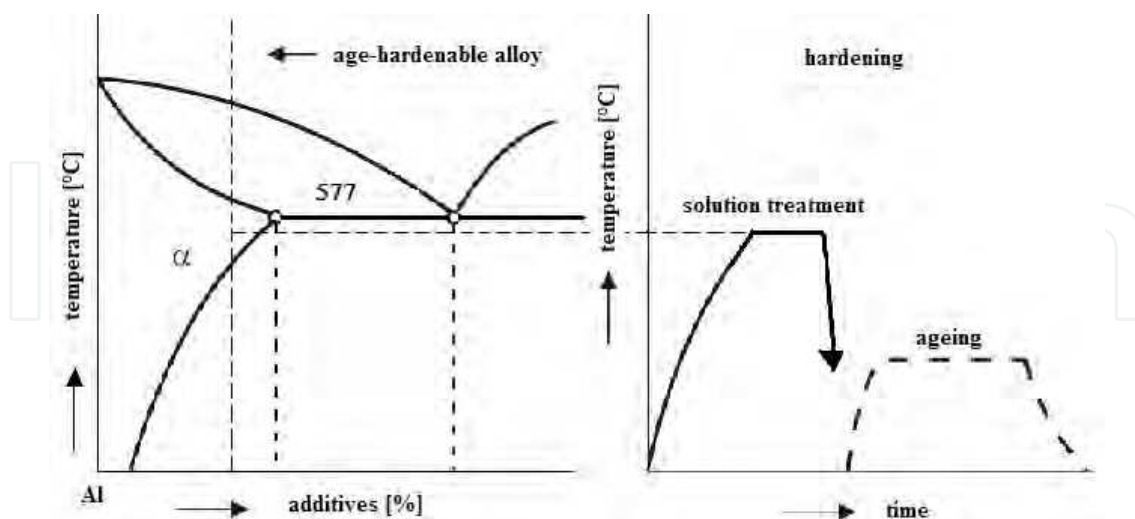


Fig. 7. The schematic diagram of hardening process for Al-Si-Cu cast alloy

Although the morphology, the amount and the distribution of the precipitates during aging process significantly influence the mechanical properties, an appropriate solution treatment is a prerequisite for obtaining desirable aging effect. From this point of view, the solution

heat treatment is critical in determining the final microstructure and mechanical properties of the alloys. Thus, it is very important to investigate the effects of solution heat treatment on the alloys, before moving on to aging issues.

Solution treatment performs three roles (Li, 1996; Lasa & Rodriguez-Ibabe, 2004; Paray & Gruzleski, 1994; Moustafa et al., 2003; Sjölander & Seifeddine, 2010):

- homogenization of as-cast structure;
- dissolution of certain intermetallic phases such as  $\text{Al}_2\text{Cu}$ ;
- changes the morphology of eutectic Si phase by fragmentation, spheroidization and coarsening, thereby improving mechanical properties, particularly ductility.

For experimental work heat treatment consisted of solution treatment for different temperatures: 505 °C, 515 °C and 525 °C; rapid water quenching (40 °C) and natural ageing (24 hours at room temperature) was used.

Influence of solution treatment on mechanical properties (strength tensile -  $R_m$  and Brinell hardness - HBS) is shown in Fig. 8 and Fig. 9.

After solution treatment, tensile strength, ductility and hardness are remarkably improved, compared to the corresponding as-cast condition. Fig. 8 shows the results of tensile strength measurements. The as cast samples have a strength value approximately 204 MPa. After 2 hours the solution treatment, independently of temperature of solution treatment, strength value immediately increases. By increasing the solution holding time from 2 to 4 hours, the tensile strength increased to 273 MPa for 515 °C. With further increase in solution temperature more than 515 °C and solution treatment time more than 4 hours, tensile strength decreases during the whole period as a result of gradual coarsening of eutectic Si, increase of inter particle spacing and dissolution of the  $\text{Al}_2\text{Cu}$  phase (at 525 °C).

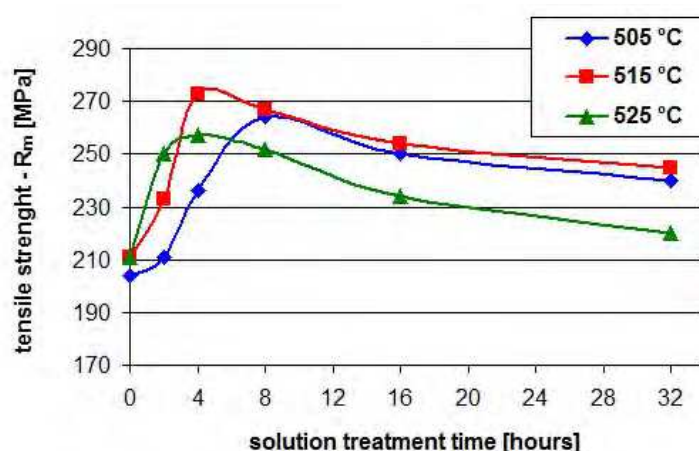


Fig. 8. Influence of solution treatment conditions on tensile strength

Fig. 9 shows the evolution of Brinell hardness value. Results of hardness are comparable with results of tensile strength. The as cast samples have a hardness value approximately 98 HB. After 2 hours the solution treatment, independently from temperature of solution treatment, hardness value immediately increases. The maximum was observed after 4 hours - approximately 124 HBS for 515 °C. However, after 8 hours solution treatment, the HB values are continuously decreasing as results of the coarsening of eutectic silicon, increase of

inter particle spacing and dissolution of the  $\text{Al}_2\text{Cu}$  phase. After prolonged solution treatment time up to 16 h at 525 °C, it is clearly that the HB values strongly decrease probably due to melting of the  $\text{Al-Al}_2\text{Cu-Si}$  phase.

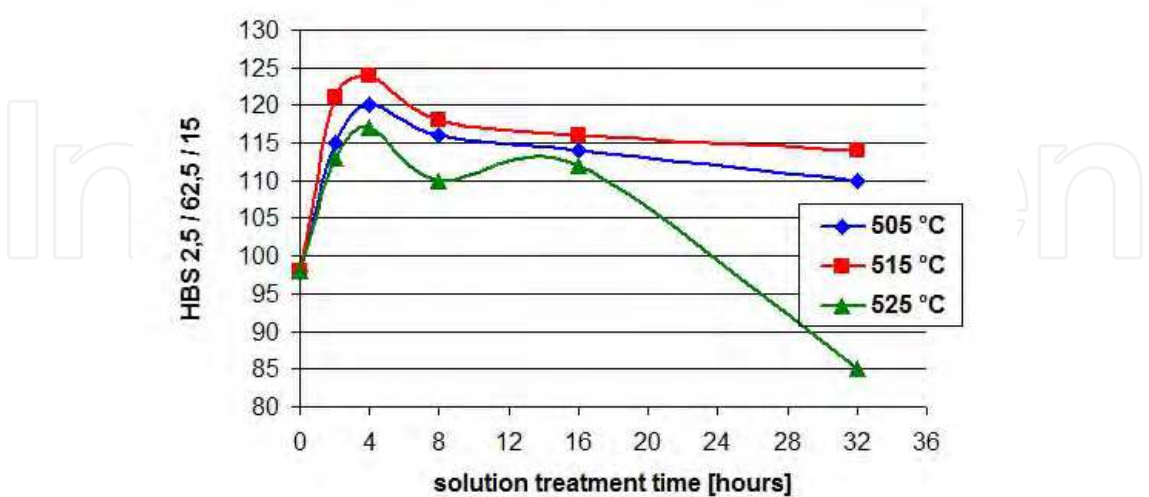
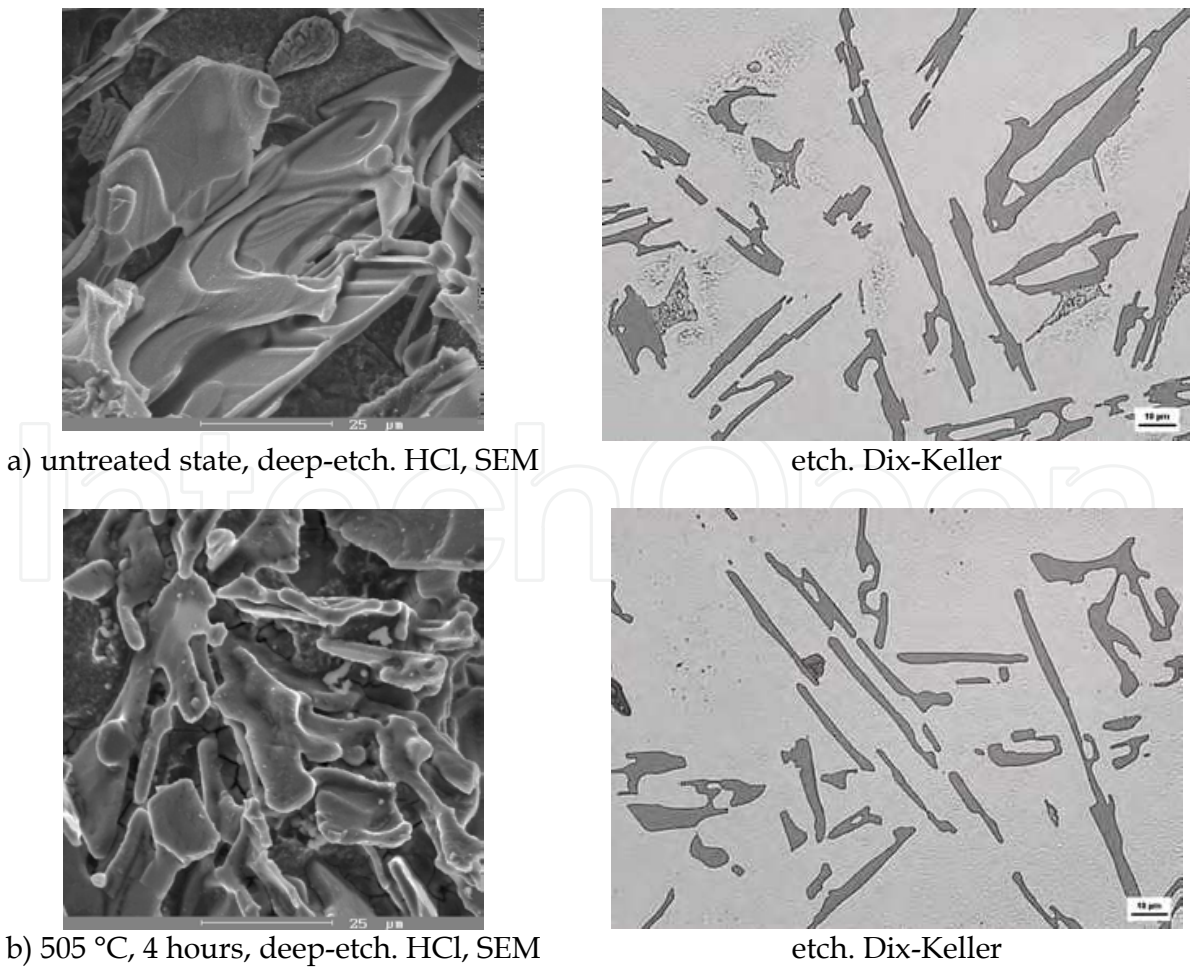
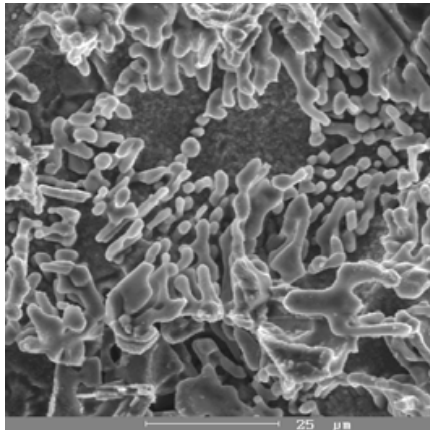


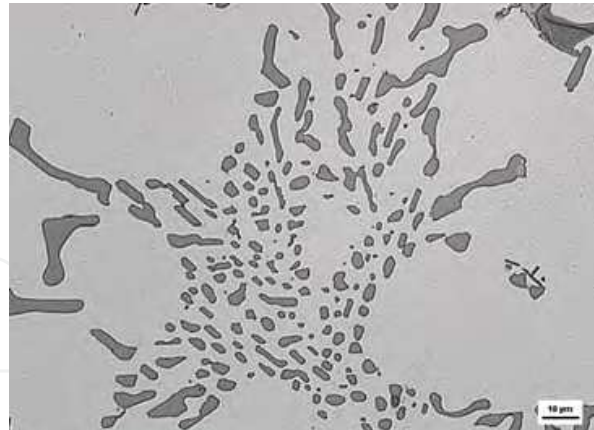
Fig. 9. Influence of solution treatment conditions on Brinell hardness



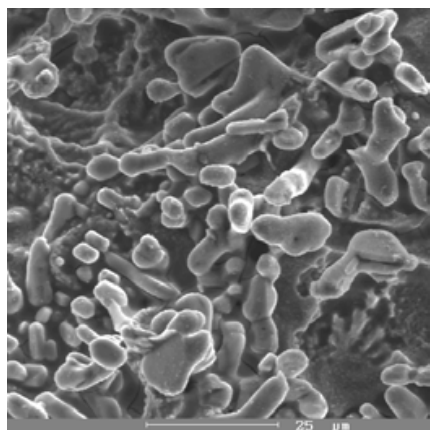




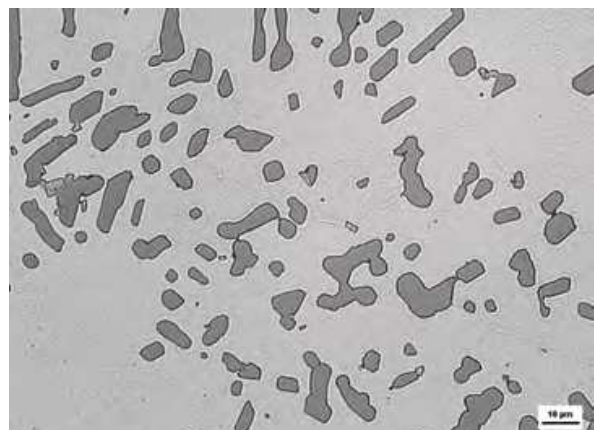
c) 515 °C, 4 hours, deep-etch. HCl, SEM



etch. Dix-Keller



d) 525 °C, 4 hours, deep-etch. HCl, SEM



etch. Dix-Keller

Fig. 10. Effect of solution treatment on morphology of eutectic Si

Obtained results (Fig. 8 and Fig. 9) suggests that to enhance the tensile strength or hardness of this recycled cast alloy by increasing of solution temperature more than 515 °C and by extending the solution time more than 4 hours does not seem suitable.

### 3.3 Effect of solution treatment on the morphology of eutectic silicon

The mechanical properties of cast component are determined largely by the shape and distribution of Si particles in the matrix. Optimum tensile, impact and fatigue properties are obtained with small, spherical and evenly distributed particles.

It is hypothesized (Paray & Gruzleski, 1994; Li, 1996; Tillova & Chalupova, 2009; Moustafa et al, 2010) that the spheroidisation process of the eutectic silicon throughout heat treatment takes place in two stages: fragmentation or dissolution of the eutectic Si branches and the spheroidisation of the separated branches. Experimental material was not modified or grain refined and so eutectic Si particles without heat treatment (untreated – as cast state) are in a form of platelets (Fig. 10a), which on scratch pattern are in a form of needles.

The solution temperature is the most important parameter that influences the kinetics of Si morphology transformation during the course of solution treatment. The effect of solution

treatment on morphology of eutectic Si, for holding time 4 hour, is demonstrated in Figures 10b, 10c and 10d. After solution treatment at the temperature of 505 °C were noted that the platelets were fragmentized into smaller platelets with spherical edges (Fig. 10b) (on scratch pattern round needles). The temperature 505 °C is for Si-spheroidisation low.

The spheroidisation process dominated at 515 °C. Si platelets fragment into smaller segments and these smaller Si particles were spheroidised to rounded shape; see Fig. 10c. By solution treatment 525 °C the spheroidised particles gradually grew larger (coarsening) (Figures 10d).

Quantitative metallography (Skocovsky & Vasko, 2007; Vasko & Belan, 2007; Belan, 2008; Vasko, 2008; Martinkovic, 2010) was carried out on an Image Analyzer NIS-Elements to quantify eutectic Si (average area of eutectic Si particle) by magnification 500 x. Figure 11 shows the average area of eutectic Si particles obtained in solution heat treated samples. This graphic relation is in line with work Paray & Gruzleski, 1994.

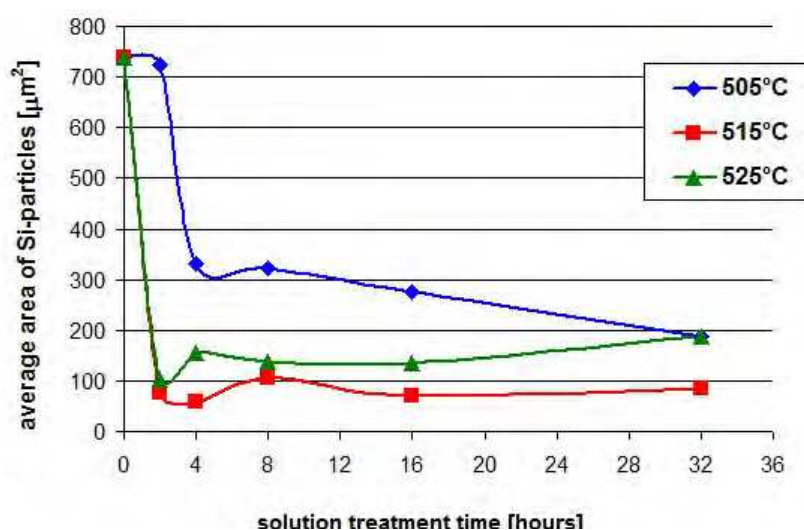


Fig. 11. Influence of solution treatment on average area of eutectic Si particles

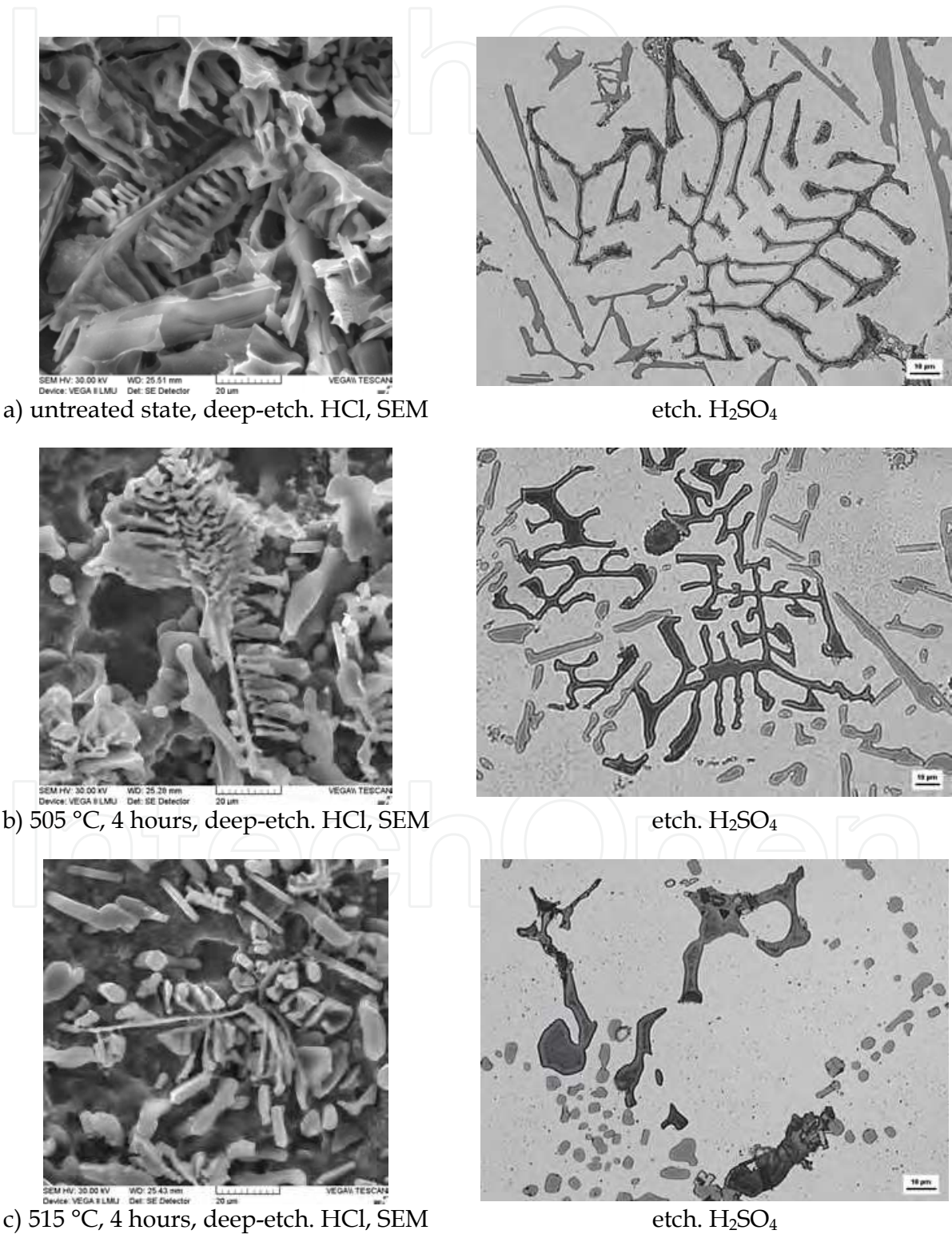
Average area of eutectic Si particles decreases with increasing solution temperature and during the whole solution period. During the two hours, the area of Si-particles decreases which indicated that they undergo fragmentation and break into smaller segments.

Minimum value of average eutectic Si particles was observed by temperature 515 °C (approximately 89 μm²). It's probably context with spheroidisation of eutectic silicon on this temperature. By solution treatment 525°C the spheroidised Si-particles in comparison with temperature 515 °C coarsen. The value of average eutectic Si particles at this temperature was observed from approximately 100 μm² (2 hour) till 187 μm² (32 hour). Prolonged solution treatment at 515°C and 525°C leads to a significant coarsening of the spheroidised Si particles.

### 3.4 Effect of solution treatment on the morphology of Fe-rich phases

The influence of iron on mechanical properties of aluminium alloys depends on the type, morphology and quantity of iron in the melt. Nevertheless, the shape of iron phases is more influential than the quantity of those iron compounds.

The evolution of the Fe-rich phases during solution treatment is described for holding time 4 hours in Fig. 12.  $\text{Al}_5\text{FeSi}$  phase is dissolved into very small needles (difficult to observe). The  $\text{Al}_{15}(\text{FeMn})_3\text{Si}_2$  phase was fragmented to smaller skeleton particles. In the untreated state  $\text{Al}_{15}(\text{FeMn})_3\text{Si}_2$  phase has a compact skeleton-like form (Fig. 12a). Solution treatment of this skeleton-like phase by  $505^\circ\text{C}$  tends only to fragmentation (Fig. 12b) and by  $515^\circ\text{C}$  or  $525^\circ\text{C}$  to fragmentation, segmentation and dissolution (Fig. 12c, Fig. 12d).





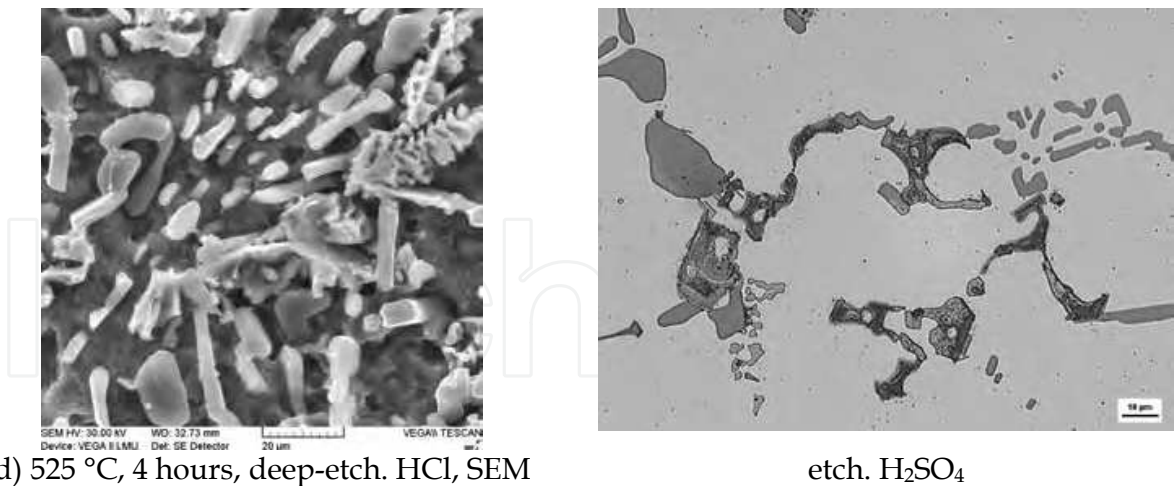


Fig. 12. Effect of solution treatment on morphology of Fe-rich phases

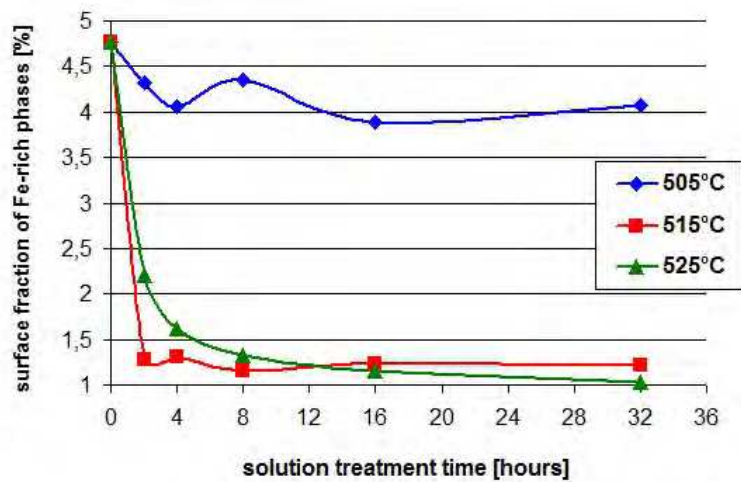


Fig. 13. Influence of solution treatment on surface fraction of Fe-rich phases

Quantitative metallography was carried out on an Image Analyzer NIS-Elements to quantify Fe-phases changes, during solution treatment. It was established that the temperature increase of solution treatment was attended not only by fragmentation of  $\text{Al}_{15}(\text{FeMn})_3\text{Si}_2$  phase, but also by decrease of surface fraction of all Fe-rich phases in  $\text{AlSi9Cu3}$  alloy (Fig. 13). For the non-heat treated state the surface fraction of Fe-rich phase was c. 4.8 %, for temperature 515 °C c. 1.6 % and for 525 °C only c. 1.25 %. Solution treatment reduces its surface fraction rather than changes its morphology (Fig. 12 and Fig. 13).

### 3.5 Effect of solution treatment o the morphology of Cu-rich phases

The Cu-rich phase solidifies as fine ternary eutectic ( $\text{Al}-\text{Al}_2\text{Cu}-\text{Si}$ ) - Fig. 6. Effect of solution treatment on morphology of  $\text{Al}-\text{Al}_2\text{Cu}-\text{Si}$  is demonstrated on Fig. 14. The changes of morphology of  $\text{Al}-\text{Al}_2\text{Cu}-\text{Si}$  observed after heat treatment are documented for holding time 4 hours.  $\text{Al}-\text{Al}_2\text{Cu}-\text{Si}$  phase without heat treatment (untreated state) occurs in form compact oval troops (Figures 14a and 15a).



After solution treatment by temperature 505 °C these phase disintegrated into fine smaller segments and the amount of Al-Al<sub>2</sub>Cu-Si phase during heat treatment decreases. This phase is gradually dissolved into the surrounding Al-matrix with an increase in solution treatment time (Fig. 14b). By solution treatment by 515 °C is this phase observed in the form coarsened globular particles and these occurs along the black needles, probably Fe-rich Al<sub>5</sub>FeSi phase (Figures 14c and 15b). By solution treatment 525 °C is this phase documented in the form molten particles with homogenous shape (Fig. 14d).

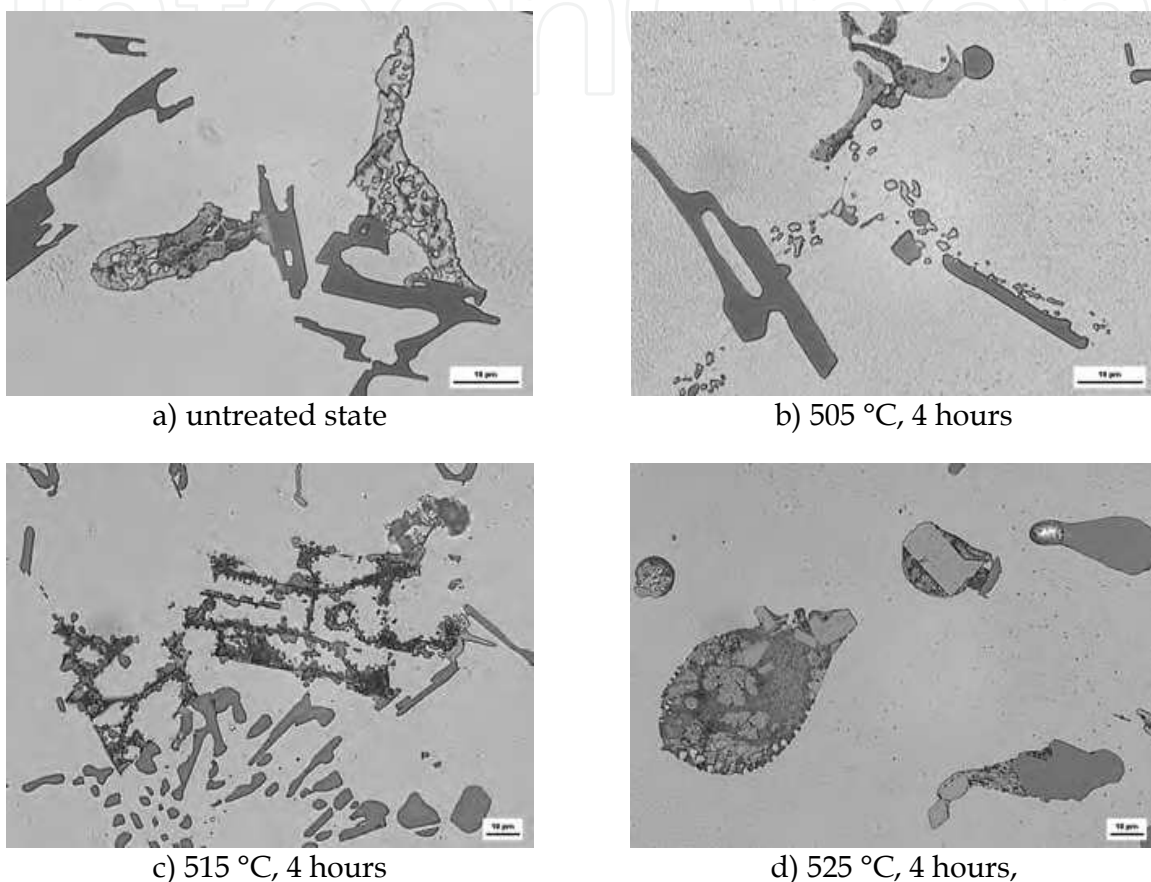


Fig. 14. Effect of solution treatment on morphology of Cu-rich phases, etch. HNO<sub>3</sub>

Compact Al-Al<sub>2</sub>Cu-Si phase disintegrates to fine separates Al<sub>2</sub>Cu particles. The amount of these phases was not obvious visible on optical microscope. On SEM microscope we observed these phases in form very small particles for every temperatures of natural aging. By observation we had to use a big extension, because we did not see these elements.

Small precipitates (Al<sub>2</sub>Cu) incipient by hardening were invisible in the optical microscope and electron microscope so it is necessary observation using TEM microscopy.

### 3.6 SEM observation of the fracture surface

Topography of fracture surfaces is commonly examined by SEM. The large depth of field is a very important advantage for fractographic investigations. Fracture surfaces of Al-Si-Cu cast alloys can be observed by means of SEM without almost any special preparation; nevertheless, if it is possible, the specimens should be examined immediately after failure

because of the very fast superficial oxidation of Al-alloys. In some cases, the specimen should be cleaned mechanically by rinsing in ultrasonic cleaner, chemical reagents, or electrolytes (Michna et al., 2007; Tillova & Chalupova, 2009; Warmuzek, 2004b).

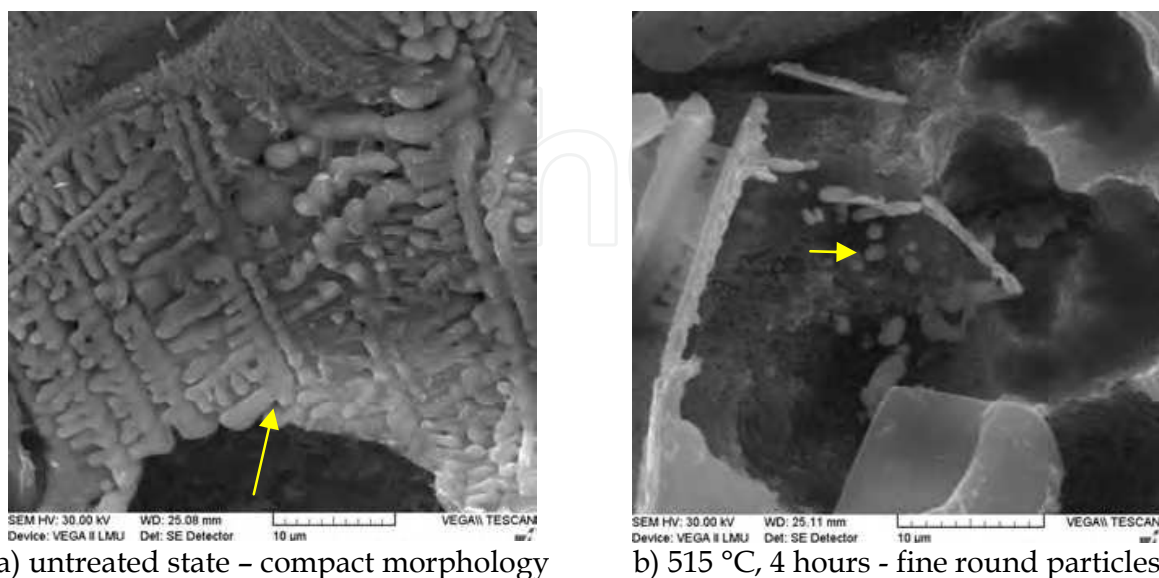


Fig. 15. Morphology of Cu-rich phases after deep etching, etch. HCl, SEM

Fractographs of the specimens in untreated state (as cast state) after impact test are documented in Fig. 16. As the experimental material was not modified and eutectic Si particles are in a form of platelets (Fig. 2), fracture surfaces are mainly composed of ductile fracture with cleavage fracture regions.

Fracture of the  $\alpha$ -matrix is transcrystalline ductile with dimples morphology and with plastically transformed walls (Fig. 16a, b). The shape of walls depends on the orientation of Si particles on fracture surface. The brittle eutectic Si and Fe-rich phases (Figures 3-5) are fractured by the transcrystalline cleavage mechanism (Fig. 16c, d, e). Cu-phase (compact ternary eutectic Al-Al<sub>2</sub>Cu-Si – Fig. 6) is fractured by transcrystalline ductile fracture with the very fine and flat dimples morphology (Fig. 16f). In some cases, to improve the contrast of the matrix/phase interface, detection of backscattered electrons (BSE) in a SEM is a very useful method (Fig. 16c). This method provides another alternative when phase attribution by morphology and/or colour, is not clearly.

Fractographs of the specimens after solution treatment are documented in Fig. 17. By temperature 505 °C of solution treatment were noted that the Si-platelets were fragmentized into smaller platelets with spherical edges (Fig. 10b). Spheroidisation process of eutectic silicon was not observed. The morphology from transcrystalline brittle fracture (cleavage) is mainly visible, but some degree of plastic deformation in the aluminium solid solution ( $\alpha$ -matrix) also may be noticed in the form of shallow dimples and plastically transformed walls (Fig. 17a, b).

After solution treatment at the 515 °C eutectic silicon is completely spheroidised (Fig. 10c). Number of brittle Fe-phases decreases (Fig. 12c). Fracture is transcrystalline ductile with fine dimples morphology (Fig. 17c, d). The size of the dimples shows the size of eutectic silicon. Local we can observe little cleavage facets of Fe-rich phases.

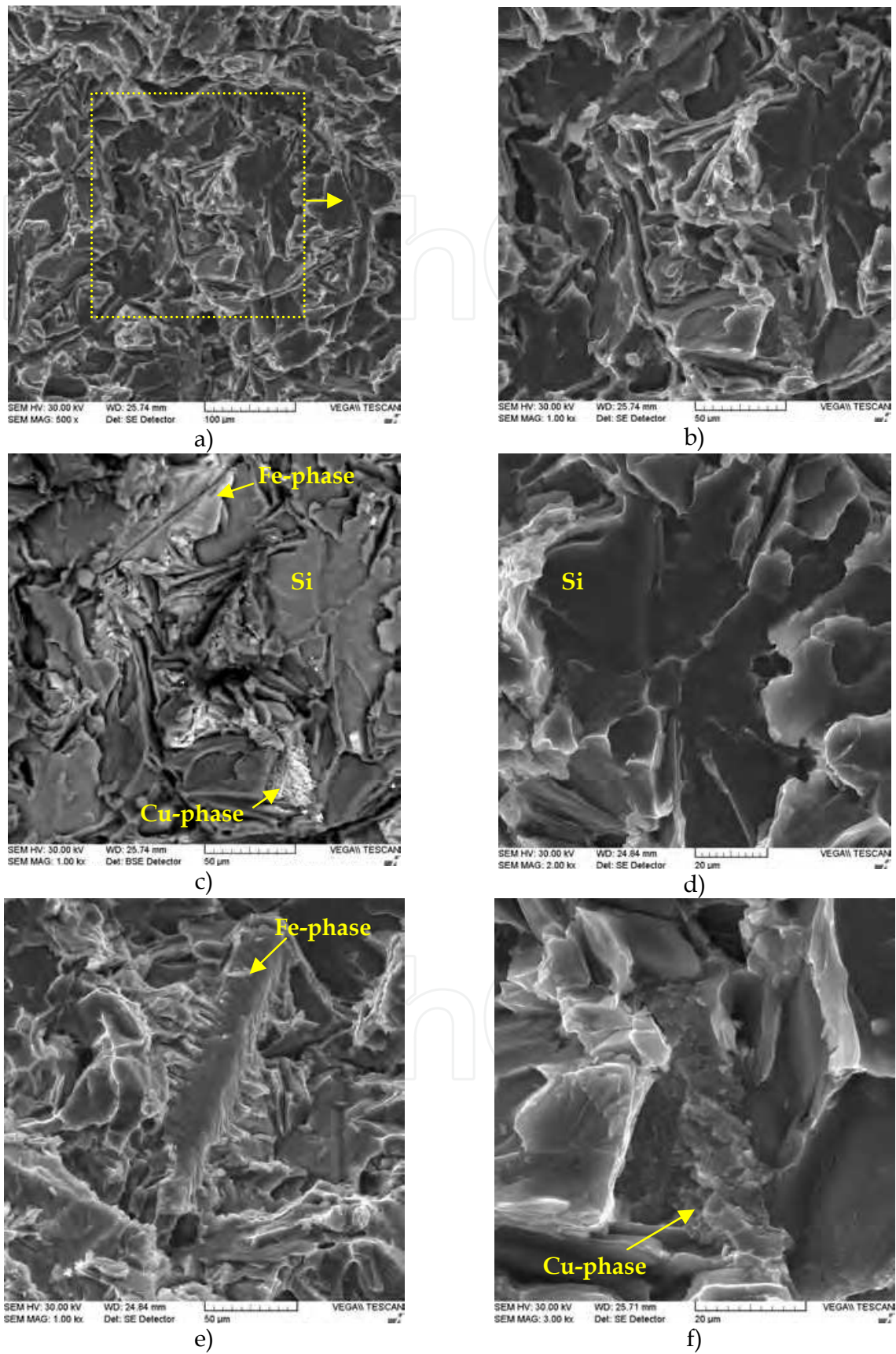


Fig. 16. Fractographs of the impact test specimen – as cast state, SEM



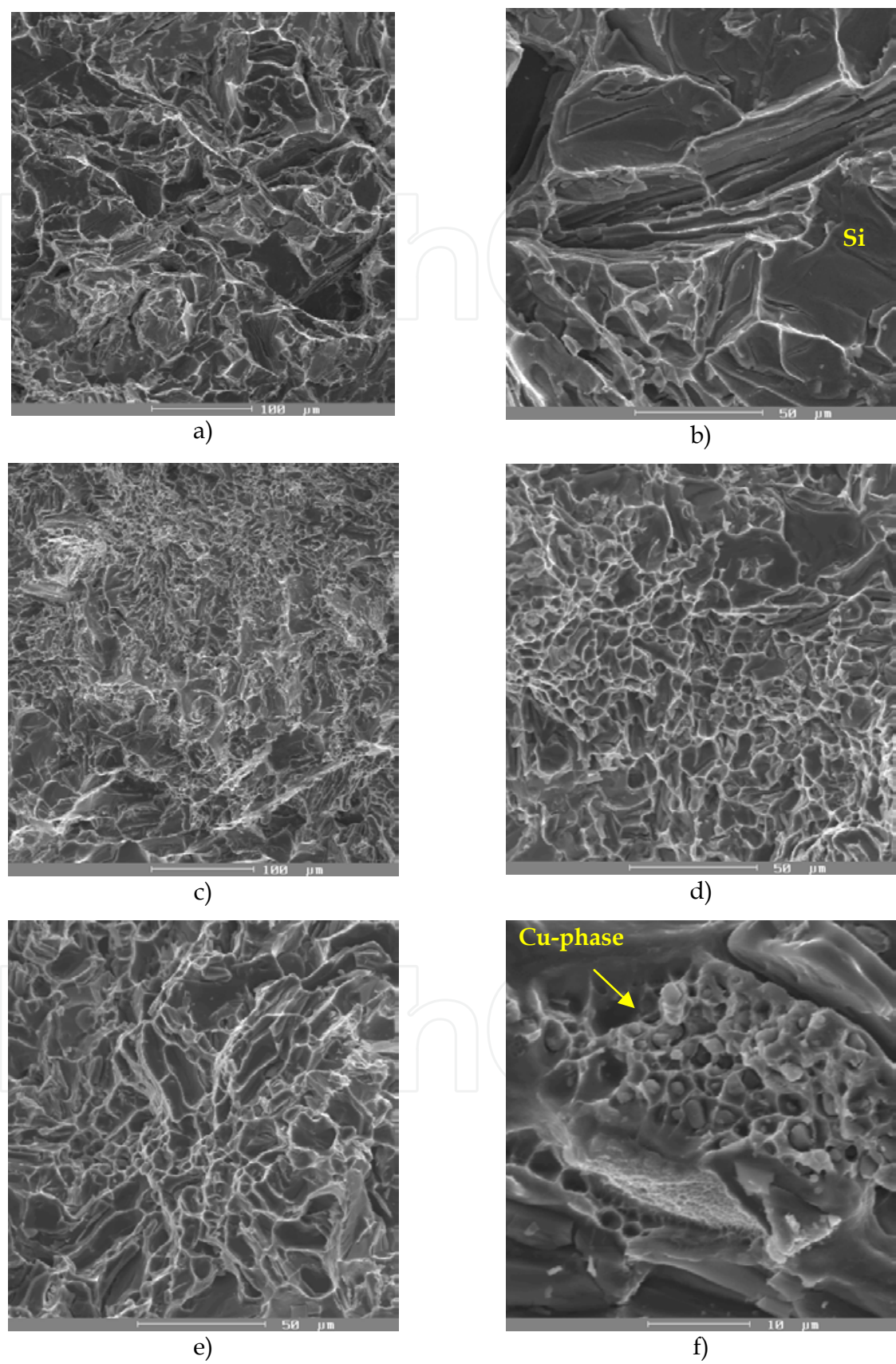


Fig. 17. Fractographs of the impact test specimen – after solution treatment, SEM



Fractograph of the specimen after solution treatment at the 525 °C is documented in Fig. 17e. Eutectic silicon is completely spheroidised too (Fig. 10d), but spheroidised Si-particles gradually grew larger. The fracture mechanism was identified as transcrystalline ductile with dimples morphology accompanied by plastically transformed walls (Fig. 17e). The size of the dimples shows the larger size of eutectic silicon as compared with fractograph Fig. 17d. Figure 17f is an example of a transcrystalline ductile fracture of Cu-rich phase after solution treatment at the 515 °C.

### 3.7 Influence of solution annealing on fatigue properties

To successfully utilize recycled Al-Si-Cu alloys in critical components, it is necessary to thoroughly understand its fatigue property too. Numerous studies have shown that fatigue property of conventional casting aluminium alloys are very sensitive to casting defects (porosity, microshrinkages and voids) and many studies have shown that, whenever a large pore is present at or near the specimen's surface, it will be the dominant cause of fatigue crack initiation (Bokuvka et al., 2002; Caceres et al., 2003; Moreira & Fuoco, 2006; Novy et al.; 2007). The occurrence of cast defects, together with the morphology of microstructural features, is strongly connected with method of casting too. By sand mould is the concentration of hydrogen in melt, as a result of damp cast surroundings, very high. The solubility of hydrogen during solidification of Al-Si cast alloys rapidly decreases and by slow cooling rates (sand casting) keeps in melt in form of pores and microshrinkages (Michna et al., 2007).

Fe is a common impurity in aluminium alloys that leads to the formation of complex Fe-rich intermetallic phases, and how these phases can adversely affect mechanical properties, especially ductility, and also lead to the formation of excessive shrinkage porosity defects in castings (Taylor, 2004; Tillova & Chalupova, 2009).

It is clear, that the morphology of Fe-rich intermetallic phases influences harmfully on fatigue properties too (Palcek et. al., 2003). Much harmful effect proves the cast defects as porosity and microshrinkages, because these defects have larger size as intermetallic phases. A comprehensive understanding of the influence of these microstructural features on the fatigue damage evolution is needed.

In the end heat treatment is considered as an important factor that affects the fatigue behaviour of casting Al-Si-Cu alloys too (Tillova & Chalupova, 2010).

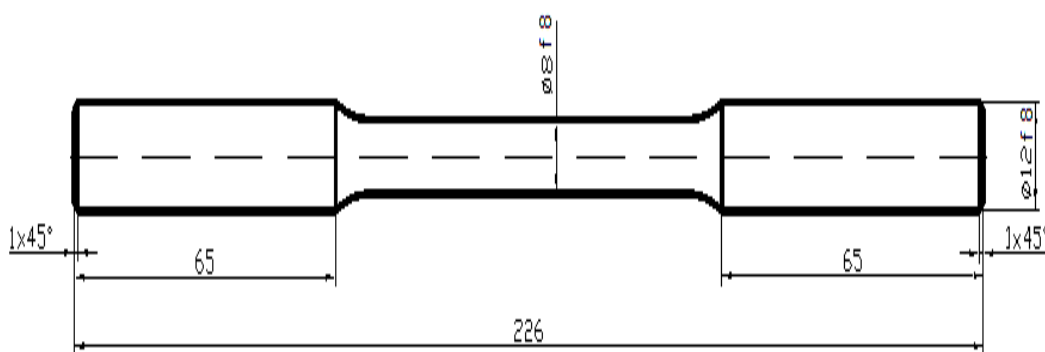


Fig. 18. Fatigue specimen geometry (all dimension in mm)

The fatigue AlSi9Cu3 tests (as-cast, solution heat treated at two temperatures 515 and 525 °C for times 4 hours, then quenched in warm water at 40 °C and natural aged at room temperature for 24 hours) were performed on rotating bending testing machine ROTOFLEX operating at 30 Hz., load ratio  $R = -1$  and at room temperature  $20 \pm 5$  °C on the air. Cylindrical fatigue specimens were produced by lathe-turning and thereafter were heat treated. Geometry of fatigue specimens is given in Fig. 18. The fatigue fracture surfaces of the fatigue - tested samples under different solution heat treatment condition were examined using a scanning electron microscope (SEM) TESCAN VEGA LMU with EDX analyser BRUKER QUANTAX after fatigue test.

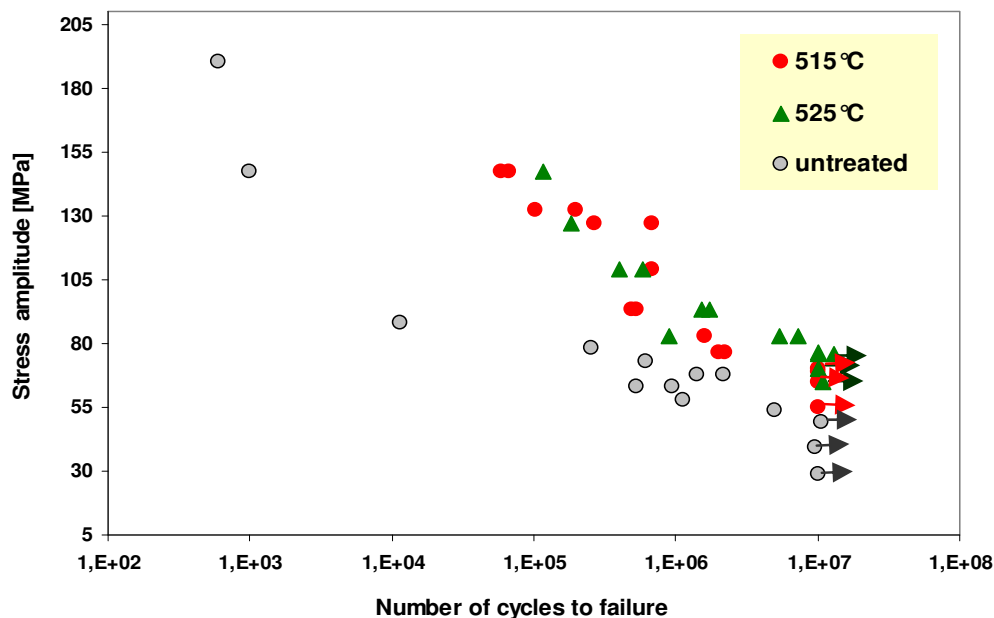


Fig. 19. Effect of solution treatment on fatigue behaviour of AlSi9Cu3 cast alloy

The untreated specimens were tested first to provide a baseline on fatigue life. In this study, the number of cycle,  $10^7$ , is taken as the infinite fatigue life. Thus, the highest applied stress under which a specimen can withstand  $10^7$  cycles is defined as the fatigue strength of the alloy. The relationship between the maximum stress level ( $S$ ), and the fatigue life in the form of the number of fatigue cycles ( $N$ ), ( $S$ - $N$  curves) is given in Fig. 19. Comparison on the fatigue properties of specimens with and without heat treatment was made. In heat untreated state has fatigue strength ( $\sigma$ ) at  $10^7$  cycles the lowest value, only  $\sigma = 49$  MPa. It is evident, that after solution treatment increased fatigue strength at  $10^7$  cycles. By the conditions of solution treatment 515 °C/4 hours the fatigue strength at  $10^7$  cycles increases up to value  $\sigma = 70$  MPa. The solution treatment by 525 °C/4 hours caused the increasing of fatigue strength at  $10^7$  cycles to value  $\sigma = 76$  MPa. The growths in fatigue strength at  $10^7$  cycles with respect to the temperature of solution treatment are 42 and 55 % respectively.

Fatigue fracture surfaces were examined in the SEM in order to find the features responsible for crack initiation. Typical fractographic surfaces are shown in Fig. 20, Fig. 21, Fig. 22 and Fig. 23. The global view of the fatigue fracture surface for untreated and heat treated specimens is very similar. The process of fatigue consists of three stages – crack initiation

stage (I), progressive crack growth across the specimen (II) and final sudden static fracture of the remaining cross section of the specimen (III) (Bokuvka et al., 2002; Palcek et al., 2003; Novy et al., 2007; Tillova & Chalupova, 2009; Moreira & Fuoco, 2006).

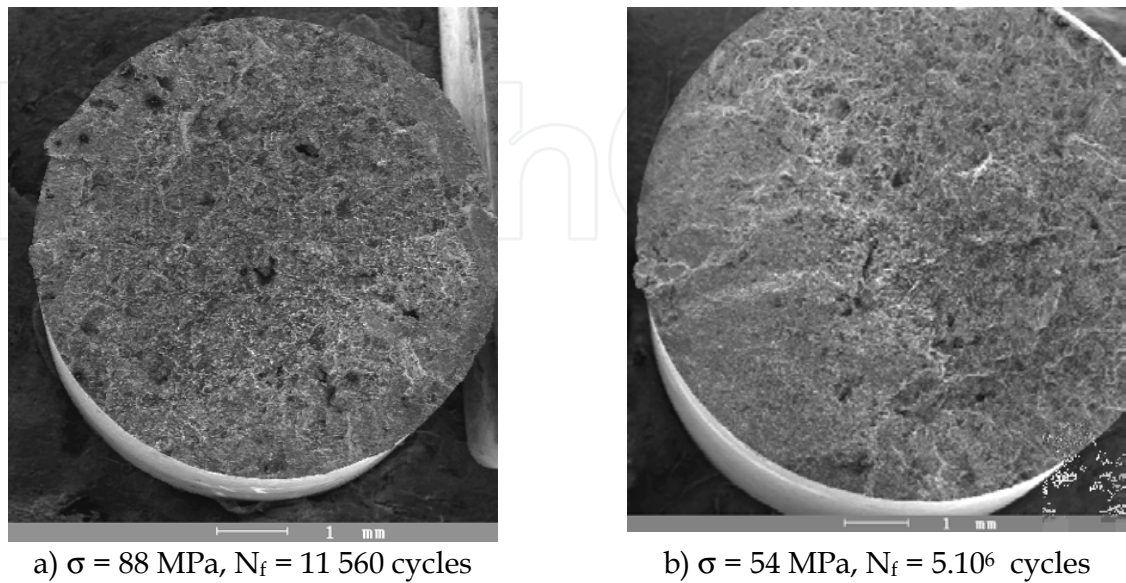


Fig. 20. Complete fracture surfaces, SEM

Stage I and II is so-called fatigue region. The three stages are directly related to the macrographic aspects of the fatigue fractures (Fig. 20). Within the bounds of fatigue tests was established that, high stress amplitude caused small fatigue region (Fig. 20a) and large region of final static rupture. With the decreasing of stress amplitude increases the fatigue region of stable propagating of cracks (Fig. 20b) and the initiation places are more focused to one point simultaneously.

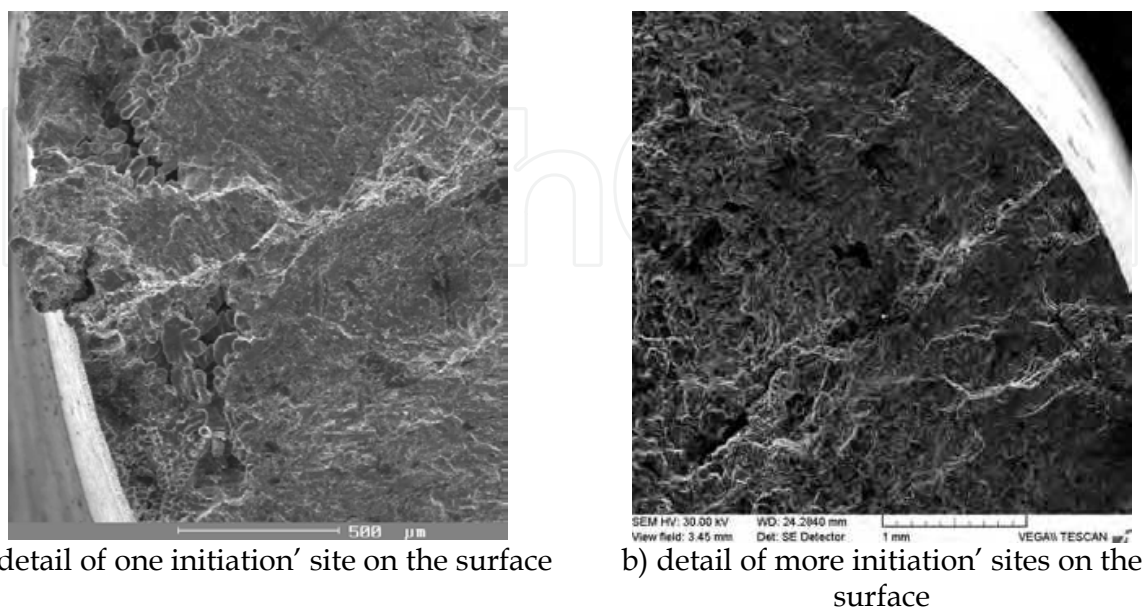


Fig. 21. Fatigue crack nucleation - overview of a fracture surface

Important to the stress concentration and to fatigue crack nucleation is the presence of casting defects as microporosities, oxide inclusions and shrinkage porosities, since the size of these defects can be much larger than the size of the microstructure particles. It was confirmed, that if are in structure marked cast defects, then behaved preferentially as an initiation's places of fatigue damage.

The cast defects were detected on the surface of test fatigue specimens. Details of the initiations site are shown in Fig. 21. For low stress amplitudes were observed one initiation place (Fig. 21a). For high stress amplitudes existed more initiation places (Fig. 21b). The occurrence of these cast defects (Fig. 22) causes the small solubility of hydrogen during solidification of Al-Si alloys.

The main micrographic characteristics of the fatigue fracture near the initiating site are the tear ridges (Fig. 23a-c) in the direction of the crack propagation and the fatigue striation in a direction perpendicular to the crack propagation. The striations are barely seen (Figure 23d). Fig. 23b illustrates the same fatigue surface as Fig. 23a, near the initiating site, in BSE electron microscopy. The result of BSE observation presents the contrast improvement of brittle Fe-rich intermetallic phases  $\text{Al}_{15}(\text{FeMn})_3\text{Si}_2$ .

Final rupture region for untreated and heat treated specimens is documented in Fig. 24. Fracture path is from micrographic aspect thus mostly transgranular and the appearance of the fracture surface is more flat. The fracture of the  $\alpha$ -dendritic network is always ductile but particularly depends on morphology of eutectic Si and quantity of brittle intermetallic phases (e.g.  $\text{Al}_{15}(\text{FeMn})_3\text{Si}_2$  or  $\text{Al}_5\text{FeSi}$ ).

The fracture surface of the as-cast samples revealed, in general, a ductile rupture mode with brittle nature of unmodified eutectic silicon platelets (Fig. 24a).

Fracture surface of heat treated samples consists almost exclusively of small dimples, with morphology and size that traced morphology of eutectic silicon (solution treatment resulted spheroidisation of eutectic silicon), such as those seen in Fig. 24b and Fig. 24c.

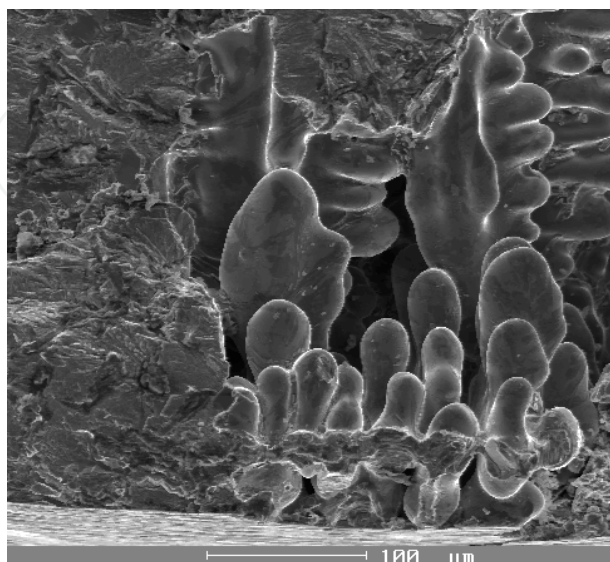
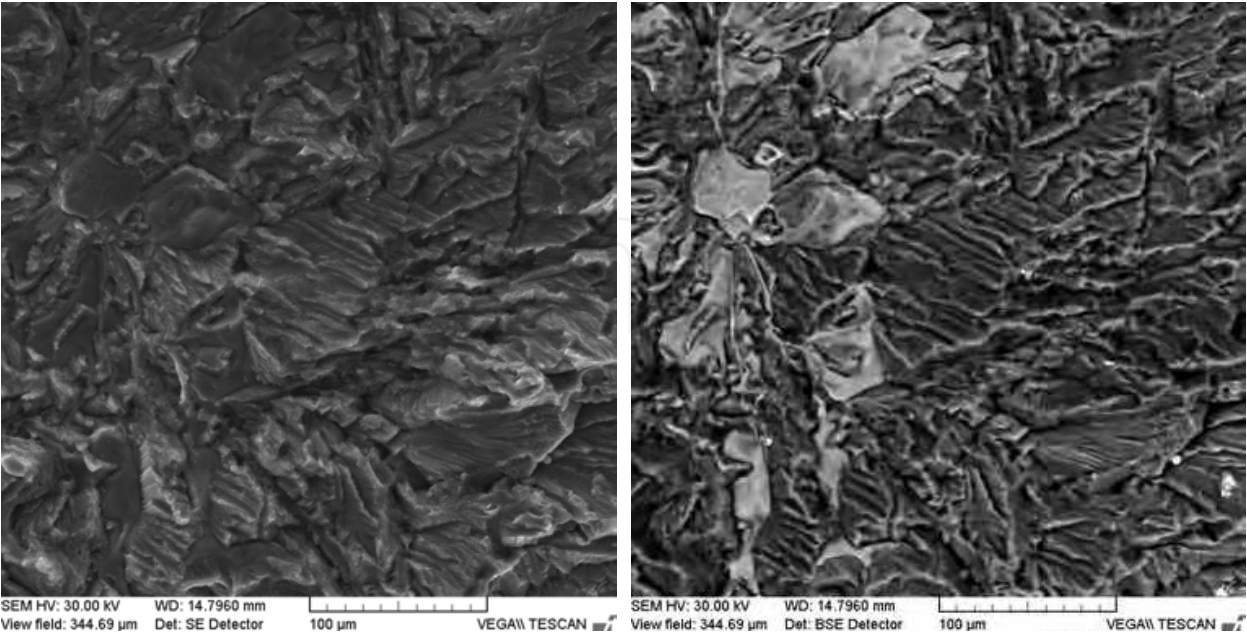
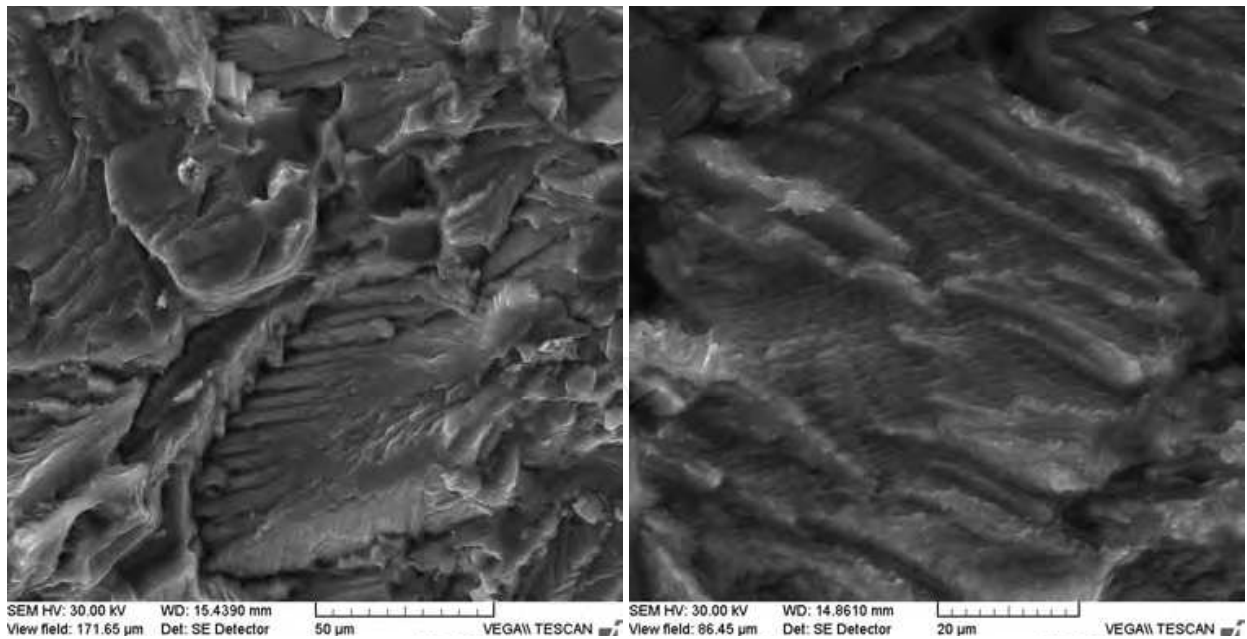


Fig. 22. Detail of cast defect





a) fatigue fracture surface near the initiating site - fine tear ridges      b) fatigue fracture surface near the initiating site - BSE



c) detail of fatigue fracture surface - tear ridges      d) detail of the typical aspect of fatigue - extremely fine striations

Fig. 23. Typical fatigue fracture surface

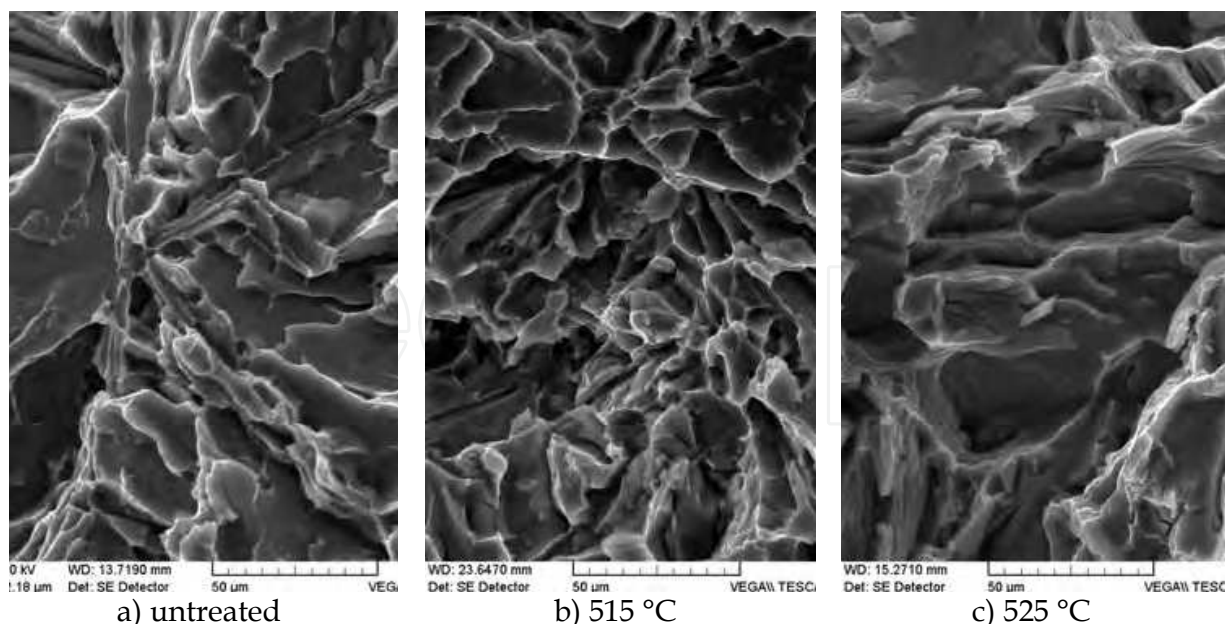


Fig. 24. Final rupture region - detail

#### 4. Acknowledgment

The authors acknowledge the financial support of the projects VEGA No1/0249/09; VEGA No1/0841/11 and European Union - the Project "Systematization of advanced technologies and knowledge transfer between industry and universities (ITMS 26110230004)".

#### 5. References

- Abdulwahab, M. (2008). Studies of the mechanical properties of age-hardened Al-Si-Fe-Mn alloy. *Australian Journal of Basic and Applied Sciences*, Vol. 2, 4, pp. 839-843
- ASM Handbook (1991). Volume 4, *Heat treating*. pp. 1861-1956, ASM International
- Belan, J. (2008). Structural Analyses of Advanced Materials for Aerospace Industry. *Materials science/Medžiagotyra*, Vol.14, 4, pp. 315-318, ISSN 1392-1320
- Bokuvka, O.; Nicoletto, G.; Kunz, L.; Palcek, P. & Chalupova, M. (2002). Low and high – frequency fatigue testing. CETRA, EDIS, Žilina, ISBN 80-8070-011-7
- Caceres, C. H.; Svenson, I. L. & Taylor, J. A. (2003). Strenght-ductility Behaviour of Al-Si-Cu-Mg Casting Alloys in T6 temper. *Int. J. Cast Metals Res.*, No. 15, pp. 531-543, ISSN 1364-0461
- Das, K. S. (2006). Designing Aluminum Alloys for a Recycle-Friendly World. *Materials Science Forum*, Vols. 519-521, pp. 1239-1244, ISSN 1662-9752
- Das, K. S. & Gren J. A. S. (2010). Aluminum Industry and Climate Change-Assessment and Responses. *JOM*, 62, 2, pp. 27-31, ISSN 1047-4838
- Dobrzański, L. A.; Maniara, R.; Krupiński, M. & Sokołowski, J. H. (2007). Microstructure and mechanical properties of AC AlSi9CuX alloys. *Journal of Achievements in Materials and Manufacturing Engineering*, Vol. 24, Issue 2, pp. 51-54, ISSN 1734-8412
- Fang, X.; Shao, G.; Liu, Y. Q. & Fan, Z. (2007). Effect of intensive forced melt convection on the mechanical properties of Fe- containing Al-Si based alloy. *Materials science and*

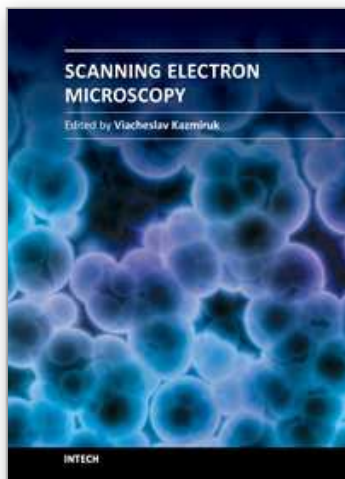
- engineering A*, Structural materials: properties, microstructure and processing. Vol. 445-446, pp. 65-72, ISSN 0921-5093
- Krupiński, M.; Labisz, K.; Rdzawski, Z. & Pawlyta, M. (2011). Cooling rate and chemical composition influence on structure of Al-Si-Cu alloys. *Journal of Achievements in Materials and Manufacturing Engineering*, Vol. 45, Issue 1, pp. 13-22, ISSN 1734-8412
- Kim, H. Y.; Park, T. Y.; Han, S. W. & Mo, L. H. (2006). Effects of Mn on the crystal structure of  $\alpha$ -Al(Mn,Fe)Si particles in A356 alloys. *Journal of Crystal Growth*, Vol. 291, Issue 1, pp. 207-211, ISSN 0022-0248
- Lasa, L. & Rodriguez-Ibabe, J. M. (2004). Evolution of the main intermetallic phases in Al-Si-Cu-Mg casting alloys during solution treatment. *Journal of Materials Science*, 39, pp. 1343-1355, ISSN 0022-2461
- Li, R. (1996). Solution heat treatment of 354 and 355 cast alloys. *AFS Transaction*, No. 26, pp. 777-783
- Li, R. X.; Li, R. D.; Zhao, Y. H.; He, L. Z.; Li, C. X.; Guan, H. R. & Hu, Z. Q. (2004). Age-hardening behaviour of cast Al-Si base alloy. *Materials Letters*, 58, pp. 2096-2101, ISSN 0167-577X
- Lu, L. & Dahle, A. K. (2005). Iron-Rich Intermetallic Phases and Their Role in Casting Defect Formation in Hypoeutectic Al-Si Alloys. *Metallurgical and Materials Transactions A*, Volume 36A, pp. 819-835, ISSN 1073-5623
- Ma, Z.; Samuel, A. M.; Samuel F. H.; Doty, H. W. & Valtierra, S. (2008). A study of tensile properties in Al-Si-Cu and Al-Si-Mg alloys: Effect of  $\beta$ -iron intermetallics and porosity. *Materials Science and Engineering A*, Vol. 490, pp. 36-51, ISSN 0921-5093
- Mahfoud, M.; Prasada Rao, A. K. & Emadi, D. (2010). The role of thermal analysis in detecting impurity levels during aluminum recycling. *J Therm Anal Calorim*, 100, pp. 847-851, ISSN 1388-6150
- Maniara, R., Dobrzański, L. A., Krupiński, M. & Sokołowski, J. H. (2007). The effect of copper concentration on the microstructure of Al-Si-Cu alloys. *Archiwes of Foundry engineering*, Vol. 7, Issue 2, pp. 119-124, ISSN 1897-3310
- Martinkovic, M. (2010). *Quantitative analysis of materials structures*. STU Bratislava, ISBN 978-80-2273-445-5 (in Slovak)
- Michna, S.; Lukac, I.; Louda, P.; Ocenasek, V.; Schneider H.; Drapala, J.; Koreny, R. ; Miskufova, A. et. al. (2007). *Aluminium materials and technologies from A to Z*. Adin, s.r.o. Presov, ISBN 978-80-89244-18-8
- Moreira, M. F. & Fuoco, R. (2006). Characteristics of fatigue fractures in Al-Si cast components. *AFS Transactions*, pp. 1-15
- Mrówka-Nowotnik, G. & Sieniawski, J. (2011). Microstructure and mechanical properties of C355.0 cast aluminium alloy. *Journal of Achievements in Materials and Manufacturing Engineering*, Vol. 47, Issue 2, pp. 85-94, ISSN 1734-8412
- Moustafa, M. A.; Samuel, F. H. & Doty, H. W. (2003). Effect of solution heat treatment and additives on the microstructure of Al-Si (A413.1) automotive alloys. *Journal of Materials Science*, 38, p. 4507-4522, ISSN 0022-2461
- Moustafa, M. A. (2009). Effect of iron content on the formation of  $\beta$ -Al<sub>5</sub>FeSi and porosity in Al-Si eutectic alloys. *Journal of Materials Processing Technology*, 209, pp. 605-610, ISSN 0924-0136



- Novy, F.; Cincala, M.; Kopas, P. & Bokuvka, O. (2007). Mechanisms of high-strength structural materials fatigue failure in ultra-wide life region. *Materials Science and Engineering A*, Vol. 462, No. 1-2, pp. 189-192, ISSN 0921-5093.
- Palcek, P.; Chalupova, M.; Nicoletto, G. & Bokuvka, O. (2003). Prediction of machine element durability. CETRA, EDIS Žilina, ISBN 80-8070-103-2
- Panuskova, M.; Tillova, E. & Chalupova, M. (2008). Relation between mechanical properties and microstructure of Al-cast alloy AlSi9Cu3. *Strength of Materials*, Vol. 40, No. 1, pp. 98-101, ISSN 1573-9325
- Paray, F. & Gruzleski, J. E. (1994). Microstructure-mechanical property relationships in a 356 alloy. Part I: Microstructure. *Cast Metals*, Vol. 7, No.1, pp. 29-40
- Rios, C. T. & Caram, R. (2003). Intermetallic compounds in the Al-Si-Cu system. *Acta Microscopica*, Vol.12, N°1, pp. 77-81, ISSN 0798-4545
- Sencakova, L. & Vircikova, E. (2007). Life cycle assessment of primary aluminium production. *Acta Metallurgica Slovaca*, 13, 3, pp. 412-419, ISSN 1338-1156
- Shabestari, S. G. (2004). The effect of iron and manganese on the formation of intermetallic compounds in aluminum-silicon alloys. *Materials Science and Engineering A*, 383, pp. 289-298, ISSN 0921-5093
- Samuel, A. M.; Samuel, F. H. & Doty, H. W. (1996). Observation on the formation  $\beta$ -Al<sub>5</sub>FeSi phase in 319 type Al-Si alloys. *Journal of Materials Science*, 31, pp. 5529-5539, ISSN 0022-2461
- Seifeddine, S. 2007. The influence of Fe on the microstructure and mechanical properties of cast Al-Si alloys. Literature review - Vilmer project. Jönköping University, Sweden
- Seifeddine, S.; Johansson, S. & Svensson, I. (2008). The Influence of Cooling Rate and Manganese Content on the  $\beta$ -Al<sub>5</sub>FeSi Phase Formation and Mechanical Properties of Al-Si-based Alloys. *Materials Science and Engineering A*, No. 490, pp. 385-390, ISSN 0921-5093
- Sjölander, E. & Seifeddine, S. (2010). Optimisation of solution treatment of cast Al-Si-Cu alloys. *Materials and Design*, 31, pp. 44-49, ISSN 0261-3069
- Skocovsky, P.; Tillova, E. & Belan, J. (2009). Influence of technological factors on eutectic silicon morphology in Al-Si alloys. *Archives of Foundry Engineering*, Vol. 9, Issue 2, pp. 169-172, ISSN 1897-3310
- Skocovsky, P. & Vasko, A. (2007). *Quantitative evaluation of structure in cast iron*, EDIS Žilina, ISBN 978-80-8070-748-4 (in Slovak)
- Taylor J. A. 2004. The effect of iron in Al-Si casting alloys. *35th Australian Foundry Institute National Conference*, pp. 148-157, Adelaide, South Australia
- Tillova, E. & Chalupova, M. (2001). Využitie hlbokého leptania pri štúdiu morfológie eutektického kremíka. *Scientific papers of the University of Pardubice, Series B - The Jan Perner Transport Faculty*, 7, pp. 41-54, ISSN 1211-6610
- Tillova, E. & Panuskova, M. (2007). Effect of Solution Treatment on Intermetallic Phase's Morphology in AlSi9Cu3 Cast Alloy. *Materials Engineering*, No. 14, pp. 73-76, ISSN 1335-0803
- Tillova, E. & Panuskova, M. (2008). Effect of Solution Treatment on Intermetallic Phase's Morphology in AlSi9Cu3 Cast Alloy. *Metallurgija/METABK*, No. 47, pp. 133-137, 1-4, ISSN 0543-5846
- Tillova, E. & Chalupova, M. (2009). *Structural analysis of Al-Si cast alloys*. EDIS Žilina, ISBN 978-80-554-0088-4, Žilina, Slovakia (in Slovak)

- Tillova, E.; Chalupova, M. & Hurtalova, L. (2010). Evolution of the Fe-rich phases in Recycled AlSi9Cu3 Cast Alloy During Solution Treatment. *Communications*, 4, pp. 95-101, ISSN 1335-4205
- Tillova, E. & Chalupova, M. (2010). Fatigue failure of recycled AlSi9Cu3 cast alloy. *Acta Metallurgica Slovaca Conference*, Vol.1, No.2, pp. 108-114, ISSN 1335-1532
- Vasko, A. & Belan, J. (2007). Comparison of methods of quantitative metallography, In: *Improvement of Quality Regarding processes and Materials*, S. Borkowski & E. Tillova, (Ed.), 53-58, PTM, ISBN 978-83-924215-3-5, Warszawa, Poland
- Vaško, A. (2008). Influence of SiC additive on microstructure and mechanical properties of nodular cast iron. *Materials science/Medžiagotyra*, Vol.14, 4, pp. 311-314, ISSN 1392-1320
- Wang, Q. G.; Apelian, D. & Lados, D. A. (2001). Fatigue Behavior of A356/357 Aluminum Cast Alloys - part II. Effect of Microstructural Constituents. *J. of Light Metals*, 1, pp. 85-97, ISSN 1471-5317
- Warmuzek, M. (2004a). Metallographic Techniques for Aluminum and Its Alloys. *ASM Handbook. Metallography and Microstructures*, Vol 9, pp. 711-751, ISBN 978-0-87170-706-2, ASM International
- Warmuzek, M. (2004b). *Aluminum-Silicon-Casting Alloys: Atlas of Microfractographs*. ISBN 0-87170-794-2, ASM International, Materials Park

IntechOpen



## **Scanning Electron Microscopy**

Edited by Dr. Viacheslav Kazmiruk

ISBN 978-953-51-0092-8

Hard cover, 830 pages

**Publisher** InTech

**Published online** 09, March, 2012

**Published in print edition** March, 2012

Today, an individual would be hard-pressed to find any science field that does not employ methods and instruments based on the use of fine focused electron and ion beams. Well instrumented and supplemented with advanced methods and techniques, SEMs provide possibilities not only of surface imaging but quantitative measurement of object topologies, local electrophysical characteristics of semiconductor structures and performing elemental analysis. Moreover, a fine focused e-beam is widely used for the creation of micro and nanostructures. The book's approach covers both theoretical and practical issues related to scanning electron microscopy. The book has 41 chapters, divided into six sections: Instrumentation, Methodology, Biology, Medicine, Material Science, Nanostructured Materials for Electronic Industry, Thin Films, Membranes, Ceramic, Geoscience, and Mineralogy. Each chapter, written by different authors, is a complete work which presupposes that readers have some background knowledge on the subject.

### **How to reference**

In order to correctly reference this scholarly work, feel free to copy and paste the following:

Eva Tillová, Mária Chalupová and Lenka Hurtalová (2012). Evolution of Phases in a Recycled Al-Si Cast Alloy During Solution Treatment, Scanning Electron Microscopy, Dr. Viacheslav Kazmiruk (Ed.), ISBN: 978-953-51-0092-8, InTech, Available from: <http://www.intechopen.com/books/scanning-electron-microscopy/evolution-of-phases-in-a-recycled-al-si-cast-alloy-during-solution-treatment>

**INTECH**  
open science | open minds

### **InTech Europe**

University Campus STeP Ri  
Slavka Krautzeka 83/A  
51000 Rijeka, Croatia  
Phone: +385 (51) 770 447  
Fax: +385 (51) 686 166  
[www.intechopen.com](http://www.intechopen.com)

### **InTech China**

Unit 405, Office Block, Hotel Equatorial Shanghai  
No.65, Yan An Road (West), Shanghai, 200040, China  
中国上海市延安西路65号上海国际贵都大饭店办公楼405单元  
Phone: +86-21-62489820  
Fax: +86-21-62489821



© 2012 The Author(s). Licensee IntechOpen. This is an open access article distributed under the terms of the [Creative Commons Attribution 3.0 License](#), which permits unrestricted use, distribution, and reproduction in any medium, provided the original work is properly cited.

IntechOpen

IntechOpen